Jyväskylän yliopiston julkaisuarkisto
Jyväskylä University Digital Archive

UNIVERSITY OF JYVÄSKYLÄ

This is an electronic reprint of the original article.
This reprint *may differ* from the original in pagination and typographic detail.

Author(s): ALICE Collaboration

Title: Measurement of the production of high-pT electrons from heavy-flavour hadron decays in Pb–Pb collisions at √sNN = 2.76 TeV

Year: 2017

Version:

Please cite the original version:

ALICE Collaboration. (2017). Measurement of the production of high-pT electrons from heavy-flavour hadron decays in Pb–Pb collisions at √sNN = 2.76 TeV. Physics Letters B, 771, 467-481. https://doi.org/10.1016/j.physletb.2017.05.060

All material supplied via JYX is protected by copyright and other intellectual property rights, and duplication or sale of all or part of any of the repository collections is not permitted, except that material may be duplicated by you for your research use or educational purposes in electronic or print form. You must obtain permission for any other use. Electronic or print copies may not be offered, whether for sale or otherwise to anyone who is not an authorised user.

Physics Letters B 771 (2017) 467–481

Contents lists available at ScienceDirect

Physics Letters B

www.elsevier.com/locate/physletb

Measurement of the production of high-p_{T} electrons from heavy-flavour hadron decays in Pb–Pb collisions at $\sqrt{s_{\mathrm{NN}}} = 2.76$ TeV

ALICE Collaboration *

ARTICLE INFO

Article history:
Received 24 October 2016
Received in revised form 12 April 2017
Accepted 24 May 2017
Available online 29 May 2017
Editor: L. Rolandi

ABSTRACT

Electrons from heavy-flavour hadron decays (charm and beauty) were measured with the ALICE detector in Pb–Pb collisions at a centre-of-mass of energy $\sqrt{s_{\mathrm{NN}}} = 2.76$ TeV. The transverse momentum (p_{T}) differential production yields at mid-rapidity were used to calculate the nuclear modification factor R_{AA} in the interval $3 < p_{\mathrm{T}} < 18$ GeV/c. The R_{AA} shows a strong suppression compared to binary scaling of pp collisions at the same energy (up to a factor of 4) in the 10% most central Pb–Pb collisions. There is a centrality trend of suppression, and a weaker suppression (down to a factor of 2) in semi-peripheral (50–80%) collisions is observed. The suppression of electrons in this broad p_{T} interval indicates that both charm and beauty quarks lose energy when they traverse the hot medium formed in Pb–Pb collisions at LHC.

© 2017 The Author. Published by Elsevier B.V. This is an open access article under the CC BY license (http://creativecommons.org/licenses/by/4.0/). Funded by SCOAP[3].

1. Introduction

High-energy heavy-ion collisions provide a unique opportunity to study the properties of the hot and dense strongly-interacting system composed of deconfined quarks and gluons – the quark-gluon plasma (QGP). The formation of a QGP is predicted by lattice QCD calculations [1–4]. A crossover transition from hadronic matter at zero baryochemical potential is expected to take place once the system temperature reaches values above $T \approx 155$ MeV and/or the energy density above $\varepsilon \approx 0.5$ GeV/fm^3 [5,6]. To characterise the physical properties of this short-lived QGP (lifetime of about 10 fm/c [7]) experimental studies use auto-generated probes, such as high-energy partons created early in the collision, thermally emitted photons, and particle correlations sensitive to the collective expansion and the dynamics of the system.

In particular, the interaction of high-p_{T} partons with the QGP, leading to modifications of the internal jet structure (jet quenching), was first proposed in [8] and is studied as a sensitive probe of the medium properties [9]. Jet quenching was first observed experimentally via the strong suppression of high transverse momentum particle production in heavy-ion collisions at the Relativistic Heavy Ion Collider (RHIC) [10–13]. Similar observations have since been reported by the Large Hadron Collider (LHC) experiments at collision energies larger by one order of magnitude with hadrons [14–16] and extended to fully reconstructed jets [17–19].

Heavy flavours (charm and beauty) are sensitive tools for studies of the in-medium parton energy loss, providing qualitatively different sensitivity to the medium properties as compared to gluon or light-quark induced jets [20,21]. The production of heavy quarks is well understood in terms of the perturbative QCD (pQCD) formalism. Good agreement between the theoretical calculations and measurements of various heavy-flavour particle production cross sections in hadronic collisions is established over a wide range of centre-of-mass energies from RHIC [22–24], through the Tevatron [25–27] to the LHC [28–32].

Interactions between partons and the medium can occur via both inelastic (radiative parton energy loss) [33–35] and elastic (collisional energy loss) [36–39] processes that depend on the parton type and the properties of the medium. The interactions with the medium modify the radiation pattern of the shower by inducing longitudinal drag (and associated longitudinal diffusion), transverse diffusion, and enhanced splitting of the propagating partons. On average, for a given parton energy, gluons are expected to lose more energy than quarks due to the difference in the Casimir colour factor [40] controlling the strength of the coupling to the coloured medium. Moreover, the energy loss is predicted to depend on the mass of the quark [41–45]. In particular, for quarks with energies comparable to their mass the radiative energy loss is expected to be smaller than for more highly-energetic partons. Consequently the relative role of elastic processes for heavy quarks is enhanced and the heavy quarks of moderate energies are expected to be more sensitive, as compared to light quarks, to the longitudinal drag and diffusion coefficients [39] that are proportional to the inverse of the mass of the parton. Moreover, as a result of multiple elastic collisions and possible in-medium resonant interactions within the hot matter, low-momentum heavy quarks could reach thermalisation in the medium [46].

* *E-mail address:* alice-publications@cern.ch.

http://dx.doi.org/10.1016/j.physletb.2017.05.060
0370-2693/© 2017 The Author. Published by Elsevier B.V. This is an open access article under the CC BY license (http://creativecommons.org/licenses/by/4.0/). Funded by SCOAP[3].

The predicted hierarchy of energy loss $\Delta E_g > \Delta E_{\text{light-q}} > \Delta E_{\text{charm}} > \Delta E_{\text{beauty}}$ [41] motivated experimental studies of the suppression patterns of heavy-flavour hadrons and their decay products. Up to now the in-medium energy loss of heavy flavours at the LHC has been studied via open charm measurements of prompt D mesons [47,48], heavy-flavour decay muon measurements at forward rapidity [31], non-prompt J/ψ, and measurements of b-jet production [49]. At RHIC the nuclear modification of heavy-flavour production has been studied via its semileptonic decays [50,51] and via measurements of D mesons [52]. The measurement that we report covers the electron (electron and positron) p_T interval 3–18 GeV/c, probing at high p_T the in-medium interaction of b quarks with momentum of a few tens of GeV/c.

The modifications of particle yields are quantified using the nuclear modification factor R_{AA}. It is constructed by dividing the p_T-differential yield in nucleus–nucleus (AA) collisions, dN_{AA}/dp_T, by the cross section in pp collisions, $d\sigma_{pp}/dp_T$, scaled by the average of the nuclear overlap function $\langle T_{AA}\rangle$ for the considered centrality class [53]

$$R_{AA} = \frac{dN_{AA}/dp_T}{\langle T_{AA}\rangle d\sigma_{pp}/dp_T}. \quad (1)$$

By construction, R_{AA} is unity when no nuclear effects are present. R_{AA} values consistent with unity have been measured for colour neutral particles (direct photons, W and Z bosons) in Pb–Pb collisions at $\sqrt{s_{NN}} = 2.76$ TeV [54–58] as well as for charged particles and heavy-flavour production in p–Pb collisions at $\sqrt{s_{NN}} = 5.02$ TeV [59–61].

This paper reports on the suppression ($R_{AA} < 1$) of electrons from semi-leptonic decays of charm and beauty hadrons measured at high-transverse momentum ($p_T > 3$ GeV/c) at mid-rapidity ($|y| < 0.6$) in Pb–Pb collisions at $\sqrt{s_{NN}} = 2.76$ TeV using the ALICE detector. The suppression is measured as a function of collision centrality and p_T in the interval $3 < p_T < 18$ GeV/c. The next two sections of the paper define the experimental setup and the analysis details together with the discussion of systematic uncertainties on the measured electron spectra. The electron yields measured in bins of centrality defined as fractions of the total hadronic cross-section of Pb–Pb collisions are then presented. Finally the p_T-differential R_{AA} in the 0–10%, 10–20%, 20–30%, 30–40%, 40–50% and 50–80% centrality classes are presented and compared to the measurement of muons from heavy-flavour hadron decays at forward rapidities [31] as well as to calculations of in-medium energy loss of heavy quarks.

2. Apparatus, data sample and analysis

2.1. Detector setup

The measurements were carried out using the ALICE detector at the LHC [62] with Pb-ion beams at a centre-of-mass energy of $\sqrt{s_{NN}} = 2.76$ TeV. A complete description of the experimental setup and the performance of detectors can be found in [63,64]. Particle track reconstruction and particle identification were performed based on information from the Inner Tracking System (ITS), the Time Projection Chamber (TPC), and the Electromagnetic Calorimeter (EMCal), located inside a solenoid magnet, which generates a 0.5 T field parallel to the beam direction. The event centrality determination was based on the signals from the V0 detector, which is a set of scintillator arrays. Moreover, the V0 detector together with the neutron Zero-Degree Calorimeters (ZN) was used for triggering and beam background rejection.

The ITS is composed of six cylindrical layers: two Silicon Pixel Detectors (SPD), two Silicon Drift Detectors (SDD), and two Silicon Strip Detectors (SSD). The SPD barrel consists of staves distributed in two layers around the beam pipe at radius of 3.9 cm and 7.6 cm, covering a length of 28.2 cm in the z direction. The outermost layer of the ITS (SSD) is located 43 cm from the beam axis.

The TPC with a radial extent of 85–247 cm, enables charged particle tracking beyond the ITS and particle identification via the measurement of the particle specific ionisation energy loss within the Ne–CO_2 gas mixture. The TPC provides up to 159 independent space points per particle track.

Charged particle tracks are reconstructed in the TPC from $p_T \approx 0.15$ GeV/c, $|\eta| < 0.9$ and full azimuth. Using the ITS and TPC space points the particle momentum is determined from the combined track fit with a resolution of about 1% at 1 GeV/c and about 3% at 10 GeV/c [64].

The front face of the EMCal is positioned at about 450 cm from the beam axis in the radial direction and the detector is approximately 110 cm deep. The detector is a layered Pb-scintillator sampling calorimeter covering 107 degrees in azimuth and a pseudorapidity region $|\eta| < 0.7$. The calorimeter design incorporates on average a moderate active volume density that results in a compact detector of about 20 radiation lengths.

The V0 detector consists of two arrays of 32 scintillator tiles placed at distances $z = 3.4$ m (V0-A) and $z = -0.9$ m (V0-C) from the nominal interaction point. V0-A and V0-C cover the full azimuth, and pseudorapidity intervals of $2.8 < \eta < 5.1$ and $-3.7 < \eta < -1.7$, respectively. The detector was used for triggering and event centrality determination.

The ZN are two identical sets of forward hadronic calorimeters which are located on both sides relative to the interaction point at $z \approx 114$ m.

2.2. Event sample and trigger

The data sample used for this analysis was collected in 2011 and it consists of $14 \cdot 10^6$ most central collisions (0–10%) and $13 \cdot 10^6$ semi-central collisions (10–50%) recorded with a minimum-bias trigger, and $3.2 \cdot 10^6$ collisions (0–90%) triggered with the EMCal. The minimum-bias trigger was a coincidence of signals from the V0-A and V0-C detectors. The timing resolution of the V0 system is better than 1 ns and it provides an efficient discrimination of the beam–beam collisions from the background events produced upstream of the experiment. Additional suppression of the background was provided by timing information from the ZDC. The minimum-bias trigger included two trigger classes for most-central and semi-central collisions, which were selected online by applying thresholds on the V0 signal amplitudes.

The EMCal provides two hierarchically-configured trigger levels (Level-0 and Level-1). For this analysis the data were recorded with the L1 trigger in coincidence with the V0 minimum-bias trigger. The trigger logic of the Level-1 trigger employed a sliding window algorithm of 4×4 towers with a sliding step of 2 towers along either of the surface axes. An event was rejected unless the energy summed within at least one set of the 16 adjacent towers was greater than a threshold. Additionally, the trigger logic was configured to adjust the online threshold according to the event centrality estimated from the analogue sum of the V0 detector signals. The threshold was adjusted such that the rejection rate was approximately constant as a function of the event centrality. The thresholds varied from 7 GeV in 10% most central events to 2 GeV in the most peripheral events.

The offline selection retained only events where the coordinate of the reconstructed vertex along the beam direction was within ±10 cm around the nominal interaction point. The event vertex reconstruction is fully efficient for the event centralities considered in this analysis.

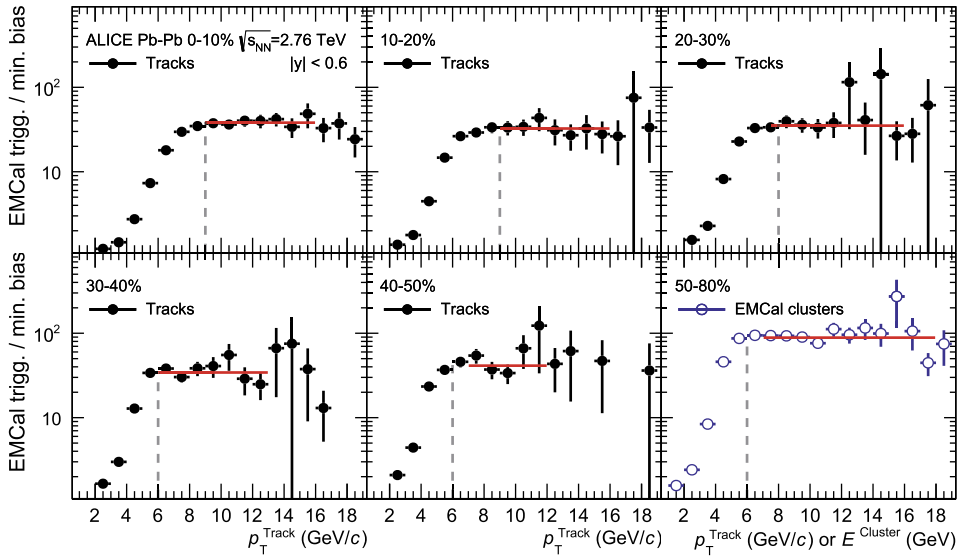

Fig. 1. Trigger turn-on curves: the ratio of inclusive electrons in EMCal triggered events to minimum-bias events as a function of associated track p_T in centrality bins between 0% and 50%. The lower right panel shows a similar ratio obtained with EMCal clusters for centrality 50–80%. The p_T from which the spectra from the minimum-bias trigger to the EMCal trigger are used are indicated with black dashed lines. The scaling factors which were obtained by fits (red lines) are summarised in Table 1. (For interpretation of the references to colour in this figure, the reader is referred to the web version of this article.)

Collisions were classified into different centrality classes in terms of percentiles of the hadronic Pb–Pb cross section using the signal amplitudes in the V0 detector. The event centrality was related to the nuclear overlap function T_{AA} via a Glauber model [65]. Details on the centrality determination can be found in [53].

To obtain the inclusive electron spectra utilising minimum bias and EMCal triggers, in each centrality class, the per-event yield of electrons from the EMCal triggered sample was scaled to the minimum-bias yield by normalisation factors determined with a data-driven method. Fig. 1 shows the ratio of p_T-differential yields of the electron candidate tracks from the EMCal triggered sample to the minimum-bias trigger sample as a function of the track p_T. The electron candidates were selected based on the ionisation energy loss in the TPC gas and the ratio of the EMCal cluster energy and the momentum of the particle track (details of electron identification are given in the next section). Because of the limited electron yield in the semi-peripheral event class (50–80%) the correction for the trigger enhancement in that interval was obtained as the ratio of the energy distributions of EMCal clusters for the two trigger types (shown in panel (f) of Fig. 1). The inclusive p_T spectrum of electrons is formed by the electron spectrum from minimum-bias events below the trigger plateau (indicated by dashed lines in Fig. 1) and the spectrum measured with only the EMCal trigger in the plateau region. The difference in the shape of the curves in Fig. 1 for p_T below the plateau is a consequence of the particle mixture contributing to the EMCal clusters and response of the EMCal to charged hadrons. The scaling factors and the transition from the minimum-bias sample to the triggered sample were determined by fits with a constant to the high-p_T plateau regions. The scaling factors for all centrality classes as well as the p_T at which the switch from the minimum-bias to the EMCal trigger spectra occurs are summarised in Table 1. The uncertainty on the factors (also reported in Table 1) was obtained from the individual fits and therefore it is driven by the statistical uncertainty of the measured spectra. The scaling factors within centralities 0–50% were extracted using the electron tracks, whereas for centralities larger than 50% the spectrum of EMCal clusters is used. The relative difference in the scaling factors depending on whether electrons or clusters were selected was studied and shown to be below 8.5%. This difference was included in the systematic uncertainty of the measurement for all centrality classes. Table 1 corresponds to Fig. 1.

Table 1
Summary for centrality dependence of the EMCal trigger scaling factor. Middle column: trigger scaling factors (together with their absolute statistical uncertainty) extracted from the ratio of electrons (or EMCal cluster) p_T spectra in EMCal triggered and minimum-bias events. Right column: particle p_T at which the spectrum measured in minimum-bias events and EMCal triggered events are switched to form the inclusive electron p_T spectrum. See text for details.

Centrality	Scaling factor	Plateau above p_T (GeV/c)
0–10%	38 ± 2.2	9
10–20%	32 ± 3.5	9
20–30%	35 ± 2.9	8
30–40%	34 ± 2.5	6
40–50%	41 ± 5.2	6
50–80%	89 ± 3.5	6

2.3. Electron reconstruction

For the reconstruction of electrons in this analysis tracks with a minimum of 100 out of 159 possible TPC space points were retained. In addition, tracks were selected using their distance of closest approach (DCA) to the primary vertex. Accepted tracks were within $|DCA_{xy}| < 2.4$ cm in the transverse plane and $|DCA_z| < 3.2$ cm along the beam axis. Furthermore, the tracks were selected within a fiducial pseudorapidity acceptance of $|\eta| < 0.6$. Each track was required to contain at least one point measured in the SPD and at least three hits out of the maximum of six in the ITS. Moreover, the electron candidates were selected by applying a cut on the specific ionisation energy loss (dE/dx) within the TPC. The measured dE/dx was required to be between -1 to 3σ, where σ is dE/dx resolution, from the expected mean of dE/dx for electrons. This selection is hereafter indicated as $-1 < n_\sigma^{TPC} < 3$. The tracks extrapolated to the sensitive volume of the EMCal were matched with a cluster if the cluster-track residual in azimuth and pseudorapidity was within a window of $|\Delta\varphi| < 0.05$ and $|\Delta\eta| < 0.05$. Such matching criteria corresponds to an effective radius of about 6 times larger than the effective Moliere radius for EMCal, thus it is fully efficient for electron tracks with $p_T > 2$ GeV/c.

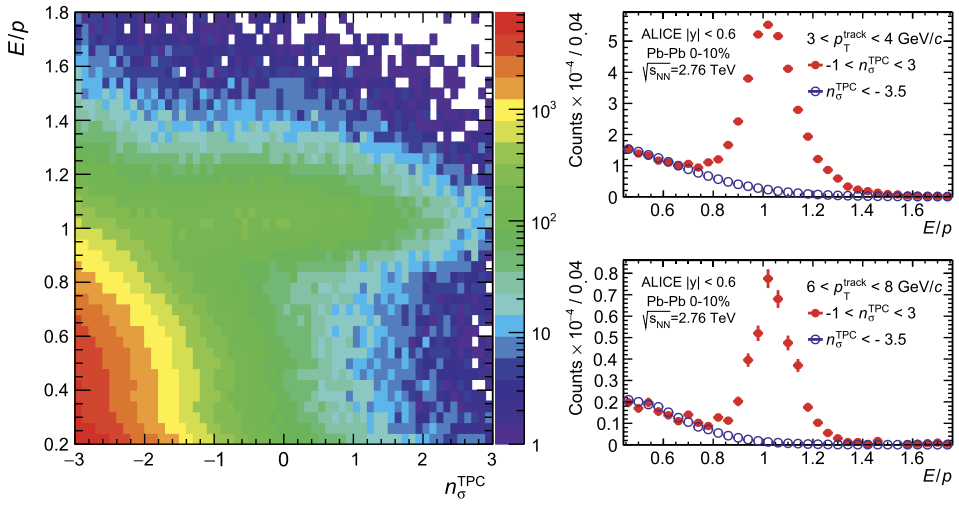

Fig. 2. ***Left:*** The ratio of E/p as a function of n_σ^{TPC} in 10% most central Pb–Pb events ($p_{\mathrm{T}} > 3$ GeV/c), where p is the charged particle momentum, E is the matched EMCal cluster energy, and σ^{TPC} is the resolution on the energy loss in the TPC gas expected for electrons. ***Right:*** E/p for electrons in two transverse momentum ranges. The blue open symbols shows the hadron contamination – an E/p distribution for particles 3.5 σ away from the mean of the true electron TPC-dE/dx distribution normalised to the electron E/p at small values of the ratio (away from the electron signal). (For interpretation of the references to colour in this figure, the reader is referred to the web version of this article.)

Additional hadron rejection used the combination of the energy deposited within EMCal and a cut on the electromagnetic shower shape [64,66]. Since the shower from an electron is fully contained and accurately measured by the EMCal, the ratio of the energy (E) measured by the EMCal and the momentum (p) for electron tracks is approximately unity ($E/p \approx 1$). The E/p distribution is qualitatively different in the case of hadrons. The E/p as a function of the n_σ^{TPC} for charged particles matched with an EMCal cluster in 10% most central events is shown in Fig. 2. From the primary tracks matched to an EMCal cluster the electron candidates were selected using a momentum independent cut of $0.9 < E/p < 1.3$. Furthermore, the shapes of the measured showers in the calorimeter can be characterised by the two eigenvalues (λ_0 and λ_1) of the covariance matrix built from the tower coordinates weighted by the logarithms of the tower energies. These eigenvalues may be used to differentiate between incident particle species [64]. A selection of $\lambda_1^2 < 0.3$, corresponding to the shorter-axis of the shower shape projected onto the EMCal surface, was applied, because the characteristic electromagnetic shower of an electron is peaked at λ_1^2 of about 0.25 independent of the cluster energy.

The remaining hadron background in the electron sample was estimated with a data-driven approach and statistically subtracted from the sample. The shape of the residual hadron background in E/p at the position of the electron peak was reconstructed using the E/p distribution for hadron-dominated tracks selected with $n_\sigma^{\mathrm{TPC}} < -3.5$. The E/p distribution of the hadrons was then normalised to match the distribution of the electron candidate in $0.4 < E/p < 0.7$ (away from the true electron peak). An example of the E/p distributions together with the estimated hadron contamination for two transverse momentum intervals is shown in the right panel of Fig. 2. The hadron contamination is less than 5% at $p_T < 10$ GeV/c in all centrality classes. At high p_T, it is larger than 10% with a maximum of about 15% at $p_T = 18$ GeV/c.

The efficiencies related to the cuts on the ionisation energy loss in the TPC were estimated with data-driven techniques [64]. The EMCal efficiencies were calculated using Monte Carlo simulations of proton-proton (PYTHIA [67]) and heavy-ion collisions (HIJING [68]) with complete detector response modelled by GEANT [69]. The product of detector acceptance and reconstruction efficiencies for inclusive electrons for the 10% most central collisions is shown in the left panel of Fig. 3. The efficiencies were estimated for each centrality class separately. A variation of about 2.5–3% was found between the most central (0–10%) and peripheral (50–80%) events.

2.4. Background electron subtraction

The main sources of electrons contributing to the inclusive electron sample in this analysis are: a) heavy-flavour hadron decay electrons; b) electrons from leptonic decays of quarkonia (J/ψ and Υ mesons); c) electrons from W and Z/γ^* decays; d) the so-called *photonic* electrons, originating from photon conversions and Dalitz decays of neutral mesons (mainly π^0 and η); and e) neutral kaon decays; however, the contribution from the non-photonic electrons created in vector meson and K_{e3} decays is negligible ($< 0.1\%$) [30] in the momentum range considered in this analysis.

The contribution of the photonic electrons to the inclusive electron sample was measured by the invariant mass method. The invariant mass distribution was determined by pairing every electron track from the inclusive sample with an oppositely-charged track selected with $-3 < n_\sigma^{\mathrm{TPC}} < 3$ to increase the chance for finding the pairs. Pairs satisfying electron identification selections and pairs satisfying a cut on the invariant mass of $m_{\mathrm{inv}} < 0.1$ GeV/c^2 were selected for further analysis. These selected unlike-sign pairs, however, contain not only true photonic electrons but also a contribution from random pairs. This combinatorial background to photonic electrons was estimated using the invariant mass distribution of the like-sign electrons ($N_{\mathrm{e}^{LS}}$), and it was subtracted from that of unlike-sign pairs ($N_{\mathrm{e}^{ULS}}$) to obtain the number of raw photonic electrons: $N_{\mathrm{e}^\gamma}^{raw} = N_{\mathrm{e}^{ULS}} - N_{\mathrm{e}^{LS}}$.

The efficiency for the identification of the photonic electrons by the invariant mass method ($\varepsilon_{\mathrm{e}^\gamma}$) was estimated from Monte Carlo simulations with full detector response and was found to be centrality independent. The efficiency, shown in the right panel of Fig. 3, is about 30% at $p_{\mathrm{T}}^e = 4$ GeV/c and rising to 55% at 18 GeV/c.

The number of photonic electrons present within the inclusive electron sample was calculated as the raw photonic electron yield corrected for the reconstruction efficiency such that: $N_{e^\gamma} = N_{e^\gamma}^{raw}/\varepsilon_{e^\gamma}$. The fraction of photonic electrons within the inclusive electron sample in the 10% most central collisions is about 30% at $p_{\mathrm{T}} = 3$ GeV/c, drops to 25% at 12 GeV/c and remains approximately constant at higher p_{T} considered in this analysis.

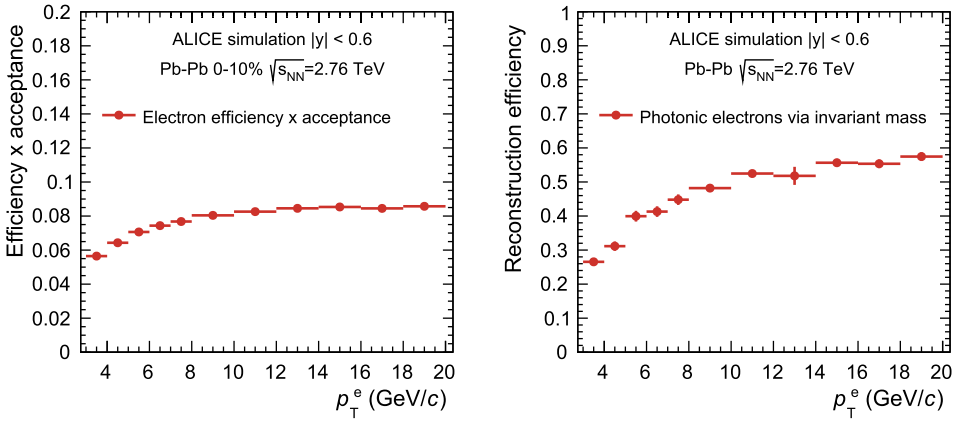

Fig. 3. ***Left:*** Product of detector acceptance and reconstruction efficiency for inclusive electrons as a function of the electron p_T. The statistical uncertainty is smaller than the size of the points. ***Right:*** Photonic electron reconstruction efficiency via invariant mass ($\varepsilon_{e\gamma}$) as a function of p_T of the electron.

The contribution to the inclusive electrons from J/ψ decays was estimated using a phenomenological interpolation at $\sqrt{s}$ = 2.76 TeV of the p_T-differential cross sections measured in pp collisions at various centre-of-mass energies [70] and scaling with the nuclear modification factor $R_{AA}^{J/\psi}$ (p_T) measured at the LHC [71,72]. In $3 < p_T < 4$ GeV/c, the contribution is 5.5% in the most central collisions and decreases at high-p_T. The contribution from Υ states estimated from the cross section measured in pp collisions [73] was found to be negligible.

The contribution of electrons from W-boson and Z/γ^* decays was estimated using the cross section obtained from the POWHEG event generator [74] for pp collisions and scaled with $\langle T_{AA} \rangle$ assuming $R_{AA} = 1$. The contribution is p_T dependent and for W-bosons it increases from 1% at 10 GeV/c to about 6% at 17 GeV/c whereas the contribution from Z/γ^* is below 1% for $p_T < 10$ GeV/c and increases to 2.4% at 17 GeV/c.

The heavy-flavour decay electron yield was reconstructed from the inclusive electron yield by first subtracting the photonic electron yield, then correcting the result of the subtraction for the efficiency, and finally, by subtracting the feed-down electrons from J/ψ and W, Z/γ^* decays.

3. Systematic uncertainties

The sources of systematic uncertainty on the reconstructed heavy-flavour decay electron p_T spectrum can be grouped into three categories:

- event selection (the event normalisation, including the scaling of the EMCal trigger events and the event centrality selection);
- electron signal extraction (uncertainties originating from corrections related to tracking and particle identification);
- non-heavy-flavour background determination.

An overview of the systematic uncertainties is presented in Table 2. For sources that depend on centrality (all but *"tracking/material"* from Table 2) the uncertainties were evaluated separately in each event class. In every case a weak centrality dependence was found (deviations of less than 3%). In the figures of Section 4 the systematic uncertainties are represented as shaded boxes around the data points.

Event normalisation. A comparison of the event normalisation obtained with the EMCal clusters and the normalisation obtained from the inclusive electrons showed a maximum deviation of 8.5%. This deviation, independent of centrality and p_T, is included as the uncertainty on the yield obtained with the triggered data. The contribution to the systematic uncertainty due to the 1.1% relative uncertainty on the fraction of hadronic cross section used in the Glauber fit to determine the centrality is less than 0.1% in the central event class (0–10%) and 3% in the semi-peripheral centrality class (50–80%) [47,75].

Table 2
Summary of systematic uncertainties on the heavy-flavour electron yields grouped according to their sources. Where applicable the uncertainty was estimated for two p_T values, 3 and 10 GeV/c (for the latter numbers are shown in parentheses). For details on the extraction of the uncertainties see text.

Source	p_T dependence (GeV/c)	Uncertainty (%)
EMCal trigger correction	only high-p_T	8.5
Centrality estimation	n/a	<0.1–3
Tracking/material	weak within 3–14	5
E/p	3 (10)	3 (3)
n_σ^{TPC}	3 (10)	3 (7)
Photonic background	3 (10)	5 (5)
J/ψ electron background	3 (10)	1 (<1)
W electron background	3 (10)	0 (<1)
Z/γ^* electron backgrounds	3 (10)	<1 (<2)

Electron identification. The systematic uncertainties on the corrections for track reconstruction, track selection and electron identification were assessed via multiple variations of the analysis selections. For each set of cuts the analysis was repeated and compared to the results obtained with the default set of cuts. These variations included changes in track quality cuts, such as the minimum number of the space points in the TPC and associated hits in the ITS. The uncertainties were estimated as a function of track p_T and for each centrality class separately. In addition, the electron identification cuts in the TPC (n_σ^{TPC}) and EMCal (E/p range) were varied around their nominal values. The uncertainty originating from the knowledge of the material budget was estimated via complete detector simulations with the radiation length varied by ±7% [76].

Subtraction of photonic background. The uncertainty on the subtracted background electrons from photon conversions and Dalitz decays was obtained by varying the invariant mass cut on the electron pairs within $0.07 < m_{inv} < 0.15$ GeV/c^2 and the minimum p_T of the tracks paired with electron candidates between 0.3 and 0.6 GeV/c.

Subtraction of electrons from J/ψ. The uncertainty on the subtracted background electrons from J/ψ decays was estimated from the experimental uncertainties on measured production yields in heavy-ion collisions [71,77].

Electrons from W and Z/γ^*. The yield of electrons from W decays was varied by ± 15% on the basis of the comparison of the W production cross section as given by the POWHEG event generator

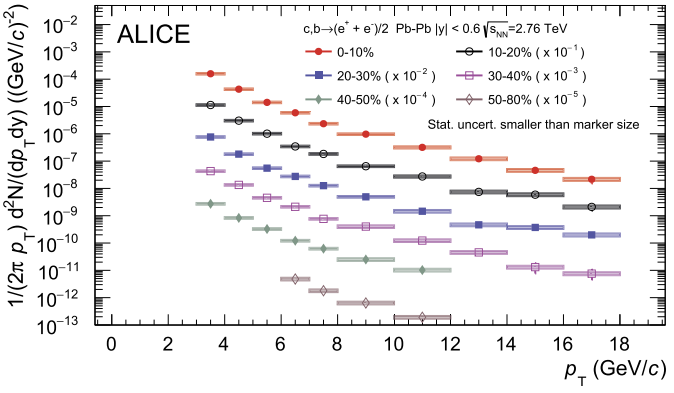

Fig. 4. Differential yields of electrons from semi-leptonic decays of heavy-flavour hadrons in classes of centrality of Pb–Pb collisions at $\sqrt{s_{\rm NN}} = 2.76$ TeV.

and the existing measurements in pp collisions at the LHC [78]. The contribution from Z/γ^* di-electron decays and its uncertainty was estimated using the POWHEG event generator and considered together with the uncertainties on the process production cross section measured in pp collisions [79]. Given the small contribution of the electrons from Z/γ^* decays to the electron spectrum of this analysis the derived uncertainty was found below 1% at the highest momentum considered.

4. Results

The $p_{\rm T}$-differential invariant yields of heavy-flavour decay electrons corrected for acceptance and efficiency in the 0–10%, 10–20%, 30–40%, 40–50% and 50–80% centrality classes in Pb–Pb collisions at $\sqrt{s_{\rm NN}} = 2.76$ TeV are shown in Fig. 4. Only the EMCal triggered data are shown for the 50–80% centrality class due to a lack of statistics in the minimum bias data sample.

The production cross section of heavy-flavour decay electrons in pp collisions at $\sqrt{s} = 2.76$ TeV, needed to compute the nuclear modification factor $R_{\rm AA}$ (Eq. (1)), was obtained from measurements and FONLL pQCD calculations [80,81]. For $p_{\rm T} < 12$ GeV/c the measurement at $\sqrt{s} = 2.76$ TeV was used [30]. For $p_{\rm T} > 12$ GeV/c there is no measurement at this energy. Thus, an extrapolated cross section was constructed from the measurement at $\sqrt{s} = 7$ TeV by the ATLAS Collaboration [82,83] and the ratio of cross sections at the two collision energies obtained from FONLL [84]. The uncertainties of the pp references are about 20% for $p_{\rm T} < 12$ GeV/c and about 15% for $p_{\rm T} > 12$ GeV/c, including the uncertainty from the scaling with $\sqrt{s}$, which was estimated by consistently varying the FONLL calculation parameters at the two energies [84].

Fig. 5 shows the resulting $R_{\rm AA}$ of heavy-flavour decay electrons for all centrality classes. The uncertainty on the average nuclear overlap function $\langle T_{\rm AA}\rangle$ for each centrality selection was taken as determined in [53]. It varies from 4% in the 10% most central events to 7% in the 50–80% centrality class, and it is shown as a box at $R_{\rm AA} = 1$ in the figure. In all cases, taking into account the $p_{\rm T}$ trend of the $R_{\rm AA}$ and the statistical uncertainties of the measurement at high-$p_{\rm T}$, the electron production yields are suppressed relative to an incoherent superposition of pp collisions. In the 10% most central events the $R_{\rm AA}$ reaches values below 0.4, while for the more peripheral events the suppression is weaker. This centrality dependence of the suppression pattern is qualitatively consistent with in-medium energy loss of heavy quarks due to a decrease of medium's initial energy density and the system size from central to peripheral collisions.

In proton–lead collisions, where formation of a hot, dense and long lived QGP is not expected, the suppression is not observed. The nuclear modification factor $R_{\rm pPb}$ measured for electrons from heavy-flavour hadron decays is consistent with unity [61]. This control measurement in p–Pb collisions confirms that the strong suppression in Pb–Pb collisions is a result of final state effects. The left panel of Fig. 6 shows the comparison between $R_{\rm pPb}$ for minimum-bias p–Pb collisions at $\sqrt{s_{\rm NN}} = 5.02$ TeV and $R_{\rm AA}$ for the 10% most central Pb–Pb collisions. The result reported here for electrons at mid-rapidity is consistent with the measurement of the suppression pattern for muons from the semi-leptonic decays of heavy-flavour hadrons at forward rapidity [31], in both, most central and semi-peripheral collisions (see Fig. 6). The lepton mea-

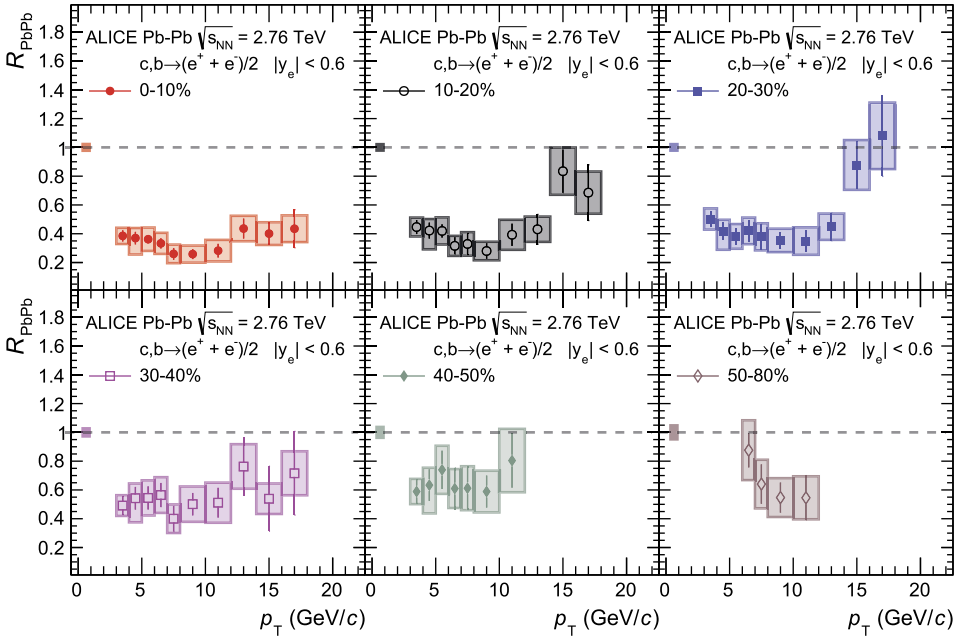

Fig. 5. $R_{\rm PbPb}$ of electrons from heavy-flavour hadron decays in centrality bins of Pb–Pb collisions at $\sqrt{s_{\rm NN}} = 2.76$ TeV. The solid band at $R_{\rm PbPb} = 1$ brackets the uncertainty on the average nuclear overlap function ($\langle T_{\rm AA}\rangle$).

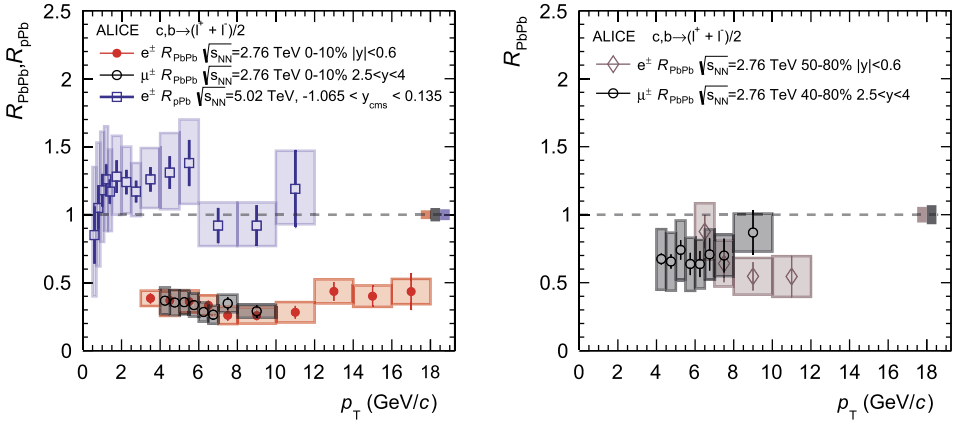

Fig. 6. ***Left:*** R_{PbPb} of electrons and muons [31] from heavy-flavour hadron decays in 10% most central Pb–Pb collisions shown together with R_{pPb} of electrons from minimum bias proton–lead collisions at $\sqrt{s_{NN}} = 5.02$ TeV [61]. ***Right:*** R_{PbPb} of electrons in semi-peripheral Pb–Pb collisions (50–80% selection for electrons and 40–80% for muons.

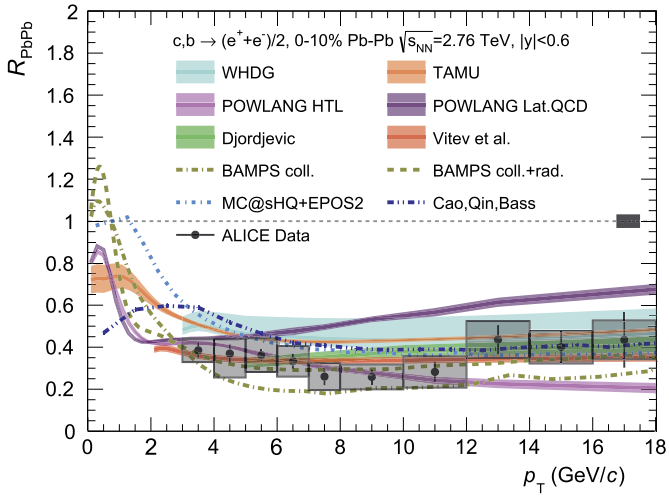

Fig. 7. R_{PbPb} of electrons from heavy-flavour hadron decays measured in 10% most central Pb–Pb collisions at $\sqrt{s_{NN}} = 2.76$ TeV compared to various theoretical calculations [86–98].

surements show remarkable similarity in the suppression pattern that, within the uncertainties, does not exhibit a rapidity dependence.

The p_T spectrum of electrons is sensitive to both charm and beauty quark energy loss. From the decay kinematics and the p_T-differential cross sections of parent hadrons with charm and beauty, it follows that electrons of p_T below 5 GeV/c are mostly sensitive to charm energy loss. On the other hand, in pp collisions a large fraction (more than 60%) of the electrons with $p_T > 10$ GeV/c originate from b-quarks [82,66,30,85,81]. The electron yield at high-p_T is therefore expected to contain a significant contribution from B mesons with p_T up to 30 GeV/c. Consequently, the strong suppression of electrons for $p_T > 10$ GeV/c is consistent with in-medium energy loss of b-quarks.

5. Comparison with models

The R_{AA} of electrons from heavy-flavour hadron decays in the most central Pb–Pb collisions is compared to theoretical models that include heavy quark interactions with the medium in Fig. 7. Most of these models were previously compared to the R_{AA} of D mesons in most central Pb–Pb collisions [75,48] as well as the positive elliptic flow of the D mesons and electrons from heavy-flavour hadron decays in semi-central Pb–Pb collisions [99,100]. We note that these models differ in the theoretical realisation of the medium properties, and of its dynamics, and also in implementations of the hadronisation and of hadron–hadron interactions in the late stages of the heavy-ion collision. Also the heavy-quark cross-section used as input to the calculation may differ between the models (PYTHIA, FONLL and POWHEG).

Djordjevic. The calculation by *Djordjevic* et al. [86] at $p_T > 5$ GeV/c is consistent with the measurement within the uncertainties including the slow increase of the R_{AA} as a function of electron p_T. The model takes into account both radiative and collisional contributions to parton energy loss. Specifically, the radiative energy loss calculations are an extension of the DGLV [101] model towards a finite size dynamical medium, finite magnetic mass, and running coupling. The model does equally well in reproducing the magnitude and p_T dependence of the D mesons R_{AA}[48].

Vitev. The calculations by *Vitev* et al. [90] also capture the magnitude of the suppression and reproduce the p_T dependence of the electrons seen in the data. The in-medium modification of the heavy quark distribution and decay probabilities are evaluated in a co-moving plasma. The predictions for heavy-flavour decay electron suppression are obtained with an improved perturbative QCD description of heavy flavour dynamics in a thermal medium where the formation and dissociation of heavy-flavour mesons are combined with parton-level charm and beauty quark radiative energy loss. The model including the dissociation of heavy-flavour hadrons captures also the suppression of D mesons.

WHDG. The band corresponding to the WHDG model calculations [87–89] is consistent with the measurement within the uncertainties; however, it systematically underpredicts the suppression below 12 GeV/c. Interestingly, the same calculation compared to the D mesons R_{AA} reproduced the data very well. The model includes elastic as well as inelastic energy loss of heavy-quarks, and the path length (geometric) fluctuations within a static thermal coloured medium with its density as the only free parameter determined via a statistical comparison of the model with the charged particle production in heavy-ion collisions.

TAMU. The R_{AA} obtained within the TAMU model of heavy quark transport within a strongly coupled thermal medium including the elastic scatterings with the medium (resonance scattering and coalescence processes) [91] underpredicts the suppression at low-p_T while it captures the magnitude of the data for $p_T > 12$ GeV/c. We note that TAMU also underpredicts the D mesons R_{AA} and its success for the electrons at high-p_T may be related to the b-quark energy loss for which the fraction from elastic processes is increased as compared to charm quarks. On the other

hand, TAMU reproduces the measured v_2 of D mesons and electrons from heavy-flavour hadron decays accurately [99,100].

BAMPS. The BAMPS [96–98] calculation, which is a partonic transport model using the Boltzmann equation, is shown for two scenarios. The *BAMPS coll.* calculation considering only the collisional energy loss in an expanding quark-gluon plasma overestimates the magnitude of the suppression within the region covered by the measurement. The calculation obtained within the same framework where both the elastic and radiative processes were considered (*BAMPS coll.+rad.*) describes the data rather well. A similar conclusion can be drawn from the comparison to the D-meson $R_{\rm AA}$. On the other hand, the *BAMPS coll.* reproduces qualitatively the v_2 of D mesons and electrons from heavy-flavour hadron decays, but the *BAMPS coll.+rad.* underestimates the D meson v_2 [99,100].

MC@sHQ+EPOS2. The results of the Monte Carlo model including a hydrodynamic calculation of the medium coupled with collisional and radiative parton energy loss *MC@sHQ+EPOS2* [93] are consistent with the measurement within the uncertainties. The model best describes the data at $p_{\rm T} > 12$ GeV/c. This model also works better for the D mesons $R_{\rm AA}$ at $p_{\rm T} > 10$ GeV/c as compared to lower momentum (meson $p_{\rm T}$ below 10 GeV/c). The authors of the model emphasise that the scattering in the hadronic phase is not present in their calculation and can have substantial effect on the low-$p_{\rm T}$ suppression and elliptic flow calculations that underpredicts the measurement [99,100].

Cao, Qin, Bass. The calculation by *Cao, Qin, and Bass* [92] reproduces the measured $R_{\rm AA}$ at high-$p_{\rm T}$ (above 12 GeV/c) while it underpredicts the suppression for low-$p_{\rm T}$. The model evaluates the dynamics of energy loss and flow of heavy quarks within the framework of a Langevin equation coupled to a (2+1)-dimensional viscous hydrodynamic model that simulates the space–time evolution of the produced hot and dense QCD matter. This calculation reproduced the suppression of D mesons very accurately, both in strength and the $p_{\rm T}$-dependence.

POWLANG. The result of the heavy-quark transport calculation using the relativistic Langevin equation with collisional energy loss, POWLANG [94,95], is shown for two choices of heavy-flavour transport coefficients within the quark-gluon plasma. In the *POWLANG HTL* [94] the coefficients are evaluated by matching the weak-coupling calculations with hard-thermal-loop (HTL) result for soft collisions with a perturbative QCD calculation for hard scatterings. This HTL variant predicts a falling trend with $p_{\rm T}$ of the electrons that is incompatible with the data and overpredicts the suppression at high momentum. Conversely, the calculation that includes the transport coefficients obtained from the Lattice QCD simulations [95] predicts the rising $R_{\rm AA}$. However, it reports larger values than the measured ones and it is incompatible with the measured magnitude of the suppression. The width of the theory curves envelopes the spread in the results of the calculation that is obtained when considering two different decoupling temperatures $T_{\rm dec}$ (155 MeV and 170 MeV) from the hydrodynamic evolution of the fireball. The relatively small width of the bands suggests a weak sensitivity of the suppression to the T_{dec}. Similar to the electron case, POWLANG HTL captures the suppression for D mesons below 5 GeV/c predicting much lower $R_{\rm AA}$ at high-$p_{\rm T}$ than observed in the data. Interestingly, as in the case of the TAMU model, the POWLANG HTL calculations provide a fair description of the D mesons v_2 measured at the LHC.

Given the level of agreement of the theoretical models with the data on v_2 and $R_{\rm AA}$ of prompt D mesons [75,48,99] and electrons from heavy-flavour decays, the following general conclusions arise:

- models incorporating the complete dynamical and thermal evolution of the medium are favoured by the data;
- the measurement indicates the need for both, collisional and radiative, energy loss of heavy quarks to be considered to explain the magnitude and the $p_{\rm T}$ dependence of the suppression.

6. Summary

The $p_{\rm T}$-differential yields of electrons from semi-leptonic decays of charm and beauty hadrons were measured at $3 < p_{\rm T} < 18$ GeV/c in several centrality classes of Pb–Pb collisions at $\sqrt{s_{\rm NN}} = 2.76$ TeV at mid-rapidity. The nuclear modification factor $R_{\rm AA}$ for the 10% most central events shows a strong suppression of electrons from heavy-flavour hadron decays. Consistent with the expectation of a decrease of the medium's initial energy density and a decreasing system size from central to peripheral collisions, the suppression is significantly weaker in more peripheral events. No significant suppression is observed in p–Pb collisions, indicating a strong in-medium energy loss of both charm and beauty quarks in Pb–Pb collisions. In particular, the strong suppression at high-momentum indicates that b-quarks lose a substantial fraction of their energy. The suppression of electrons is quantitatively consistent with measurements of $R_{\rm AA}$ of muons from semi-leptonic heavy-flavour decays in $2.5 < y < 4$, disfavouring a strong dependence of energy loss on rapidity in the range $|y| < 4$. Theoretical calculations that include collisional and radiative in-medium energy loss for both charm and beauty quarks reproduce the experimental findings. In particular, models incorporating the dynamical evolution of the medium are preferred by the data.

Acknowledgements

The ALICE Collaboration would like to thank all its engineers and technicians for their invaluable contributions to the construction of the experiment and the CERN accelerator teams for the outstanding performance of the LHC complex. The ALICE Collaboration gratefully acknowledges the resources and support provided by all Grid centres and the Worldwide LHC Computing Grid (WLCG) collaboration. The ALICE Collaboration acknowledges the following funding agencies for their support in building and running the ALICE detector: A.I. Alikhanyan National Science Laboratory (Yerevan Physics Institute) Foundation (ANSL), State Committee of Science and World Federation of Scientists (WFS), Armenia; Austrian Academy of Sciences and Nationalstiftung für Forschung, Technologie und Entwicklung, Austria; Conselho Nacional de Desenvolvimento Científico e Tecnológico (CNPq), Financiadora de Estudos e Projetos (Finep) and Fundação de Amparo à Pesquisa do Estado de São Paulo (FAPESP), Brazil; Ministry of Education of China (MOE of China), Ministry of Science & Technology of China (MOST of China) and National Natural Science Foundation of China (NSFC), China; Ministry of Science, Education and Sports and Croatian Science Foundation, Croatia; Centro de Investigaciones Energéticas, Medioambientales y Tecnológicas (CIEMAT), Cuba; Ministry of Education, Youth and Sports of the Czech Republic, Czech Republic; Danish National Research Foundation (DNRF), The Carlsberg Foundation and The Danish Council for Independent Research–Natural Sciences, Denmark; Helsinki Institute of Physics (HIP), Finland; Commissariat à l'Energie Atomique (CEA) and Institut National de Physique Nucléaire et de Physique des Particules (IN2P3) and Centre National de la Recherche Scientifique (CNRS), France; Bundesministerium für Bildung, Wissenschaft, Forschung und Technologie (BMBF) and GSI Helmholtzzentrum für Schwerionenforschung GmbH, Germany; Ministry of Education, Research and Religious Affairs, Greece; National Research, Development and Innovation Office, Hungary; Department of Atomic Energy, Government of India (DAE), India; Indonesian Institute of Science,

Indonesia; Centro Fermi – Museo Storico della Fisica e Centro Studi e Ricerche Enrico Fermi and Istituto Nazionale di Fisica Nucleare (INFN), Italy; Institute for Innovative Science and Technology, Nagasaki Institute of Applied Science (IIST), Japan Society for the Promotion of Science (JSPS) KAKENHI and Japanese Ministry of Education, Culture, Sports, Science and Technology (MEXT), Japan; Consejo Nacional de Ciencia y Tecnología (CONACYT), through Fondo de Cooperación Internacional en Ciencia y Tecnología (FONCICYT) and Dirección General de Asuntos del Personal Academico (DGAPA), Mexico; Nationaal instituut voor subatomaire fysica (Nikhef), Netherlands; The Research Council of Norway, Norway; Commission on Science and Technology for Sustainable Development in the South (COMSATS), Pakistan; Pontificia Universidad Católica del Perú, Peru; Ministry of Science and Higher Education and National Science Centre, Poland; Ministry of Education and Scientific Research, Institute of Atomic Physics and Romanian National Agency for Science, Technology and Innovation, Romania; Joint Institute for Nuclear Research (JINR), Ministry of Education and Science of the Russian Federation and National Research Centre Kurchatov Institute, Russia; Ministry of Education, Science, Research and Sport of the Slovak Republic, Slovakia; National Research Foundation of South Africa, South Africa; Korea Institute of Science and Technology Information and National Research Foundation of Korea (NRF), South Korea; Centro de Investigaciones Energéticas, Medioambientales y Tecnológicas (CIEMAT) and Ministerio de Ciencia e Innovacion, Spain; Knut & Alice Wallenberg Foundation (KAW) and Swedish Research Council (VR), Sweden; European Organization for Nuclear Research, Switzerland; National Science and Technology Development Agency (NSDTA), Office of the Higher Education Commission under NRU project of Thailand and Suranaree University of Technology (SUT), Thailand; Turkish Atomic Energy Agency (TAEK), Turkey; National Academy of Sciences of Ukraine, Ukraine; Science and Technology Facilities Council (STFC), United Kingdom; National Science Foundation of the United States of America (NSF) and United States Department of Energy, Office of Nuclear Physics (DOE NP), United States.

References

[1] H. Satz, Color deconfinement in nuclear collisions, Rep. Prog. Phys. 63 (2000) 1511, arXiv:hep-ph/0007069.
[2] S.A. Bass, M. Gyulassy, H. Stoecker, W. Greiner, Signatures of quark gluon plasma formation in high-energy heavy ion collisions: a critical review, J. Phys. G 25 (1999) R1–R57, arXiv:hep-ph/9810281.
[3] E.V. Shuryak, Theory and phenomenology of the QCD vacuum. 7. Macroscopic excitations, Phys. Rep. 115 (1984) 151.
[4] J. Cleymans, R. Gavai, E. Suhonen, Quarks and gluons at high temperatures and densities, Phys. Rep. 130 (1986) 217.
[5] S. Borsanyi, G. Endrodi, Z. Fodor, A. Jakovac, S.D. Katz, S. Krieg, C. Ratti, K.K. Szabo, The QCD equation of state with dynamical quarks, J. High Energy Phys. 11 (2010) 077, arXiv:1007.2580 [hep-lat].
[6] T. Bhattacharya, et al., QCD phase transition with chiral quarks and physical quark masses, Phys. Rev. Lett. 113 (8) (2014) 082001, arXiv:1402.5175 [hep-lat].
[7] ALICE Collaboration, K. Aamodt, et al., Two-pion Bose–Einstein correlations in pp collisions at $\sqrt{s} = 900$ GeV, Phys. Rev. D 82 (2010) 052001, arXiv:1007.0516 [hep-ex].
[8] J.D. Bjorken, Energy loss of energetic partons in quark–gluon plasma: possible extinction of high p_{T} jets in hadron–hadron collisions, FERMILAB-PUB-82-059-THY, FERMILAB-PUB-82-059-T.
[9] JET Collaboration, K.M. Burke, et al., Extracting the jet transport coefficient from jet quenching in high-energy heavy-ion collisions, Phys. Rev. C 90 (1) (2014) 014909, arXiv:1312.5003 [nucl-th].
[10] STAR Collaboration, J. Adams, et al., Experimental and theoretical challenges in the search for the quark gluon plasma: the STAR collaboration's critical assessment of the evidence from RHIC collisions, Nucl. Phys. A 757 (2005) 102–183, arXiv:nucl-ex/0501009.
[11] PHENIX Collaboration, K. Adcox, et al., Formation of dense partonic matter in relativistic nucleus–nucleus collisions at RHIC: experimental evaluation by the PHENIX collaboration, Nucl. Phys. A 757 (2005) 184–283, arXiv:nucl-ex/0410003.
[12] BRAHMS Collaboration, I. Arsene, et al., Quark gluon plasma and color glass condensate at RHIC? The perspective from the BRAHMS experiment, Nucl. Phys. A 757 (2005) 1–27, arXiv:nucl-ex/0410020.
[13] PHOBOS Collaboration, B. Back, et al., The PHOBOS perspective on discoveries at RHIC, Nucl. Phys. A 757 (2005) 28–101, arXiv:nucl-ex/0410022.
[14] ALICE Collaboration, K. Aamodt, et al., Suppression of charged particle production at large transverse momentum in central Pb–Pb collisions at $\sqrt{s_{NN}} = 2.76$ TeV, Phys. Lett. B 696 (2011) 30–39, arXiv:1012.1004 [nucl-ex].
[15] ALICE Collaboration, K. Aamodt, et al., Particle-yield modification in jet-like azimuthal di-hadron correlations in Pb–Pb collisions at $\sqrt{s_{NN}} = 2.76$ TeV, Phys. Rev. Lett. 108 (2012) 092301, arXiv:1110.0121 [nucl-ex].
[16] CMS Collaboration, S. Chatrchyan, et al., Study of high-pT charged particle suppression in PbPb compared to pp collisions at $\sqrt{s_{NN}} = 2.76$ TeV, Eur. Phys. J. C 72 (2012) 1945, arXiv:1202.2554 [nucl-ex].
[17] ATLAS Collaboration, G. Aad, et al., Observation of a centrality-dependent dijet asymmetry in lead-lead collisions at $\sqrt{s_{NN}} = 2.77$ TeV with the ATLAS detector at the LHC, Phys. Rev. Lett. 105 (2010) 252303, arXiv:1011.6182 [hep-ex].
[18] CMS Collaboration, S. Chatrchyan, et al., Observation and studies of jet quenching in PbPb collisions at nucleon–nucleon center-of-mass energy = 2.76 TeV, Phys. Rev. C 84 (2011) 024906, arXiv:1102.1957 [nucl-ex].
[19] ALICE Collaboration, J. Adam, et al., Measurement of jet suppression in central Pb–Pb collisions at $\sqrt{s_{\mathrm{NN}}} = 2.76$ TeV, Phys. Lett. B 746 (2015) 1–14, arXiv:1502.01689 [nucl-ex].
[20] A. Andronic, et al., Heavy-flavour and quarkonium production in the LHC era: from proton–proton to heavy-ion collisions, Eur. Phys. J. C 76 (3) (2016) 107, arXiv:1506.03981 [nucl-ex].
[21] F. Prino, R. Rapp, Open heavy flavor in QCD matter and in nuclear collisions, arXiv:1603.00529 [nucl-ex].
[22] PHENIX Collaboration, A. Adare, et al., Heavy quark production in $p + p$ and energy loss and flow of heavy quarks in Au+Au collisions at $\sqrt{s_{NN}} = 200$ GeV, Phys. Rev. C 84 (2011) 044905, arXiv:1005.1627 [nucl-ex].
[23] STAR Collaboration, J. Adams, et al., Open charm yields in d + Au collisions at s(NN)**(1/2) = 200-GeV, Phys. Rev. Lett. 94 (2005) 062301, arXiv:nucl-ex/0407006.
[24] STAR Collaboration, L. Adamczyk, et al., Measurements of D^0 and D^* production in $p + p$ collisions at $\sqrt{s} = 200$ GeV, Phys. Rev. D 86 (2012) 072013, arXiv:1204.4244 [nucl-ex].
[25] CDF Collaboration, D. Acosta, et al., Measurement of prompt charm meson production cross sections in $p\bar{p}$ collisions at $\sqrt{s} = 1.96$ TeV, Phys. Rev. Lett. 91 (2003) 241804, arXiv:hep-ex/0307080.
[26] D0 Collaboration, V.M. Abazov, et al., Search for scalar top quarks in the acoplanar charm jets and missing transverse energy final state in $p\bar{p}$ collisions at $\sqrt{s} = 1.96$-TeV, Phys. Lett. B 665 (2008) 1–8, arXiv:0803.2263 [hep-ex].
[27] D0 Collaboration, V.M. Abazov, et al., Measurement of B_s^0 mixing parameters from the flavor-tagged decay $B_s^0 \to J/\psi\phi$, Phys. Rev. Lett. 101 (2008) 241801, arXiv:0802.2255 [hep-ex].
[28] CMS Collaboration, S. Chatrchyan, et al., Inclusive b-jet production in pp collisions at $\sqrt{s} = 7$ TeV, J. High Energy Phys. 04 (2012) 084, arXiv:1202.4617 [hep-ex].
[29] ATLAS Collaboration, G. Aad, et al., Measurement of the inclusive and dijet cross-sections of b^- jets in pp collisions at $\sqrt{s} = 7$ TeV with the ATLAS detector, Eur. Phys. J. C 71 (2011) 1846, arXiv:1109.6833 [hep-ex].
[30] ALICE Collaboration, B.B. Abelev, et al., Measurement of electrons from semileptonic heavy-flavor hadron decays in pp collisions at $\sqrt{s} = 2.76$ TeV, Phys. Rev. D 91 (1) (2015) 012001, arXiv:1405.4117 [nucl-ex].
[31] ALICE Collaboration, B. Abelev, et al., Production of muons from heavy flavour decays at forward rapidity in pp and Pb–Pb collisions at $\sqrt{s_{NN}} = 2.76$ TeV, Phys. Rev. Lett. 109 (2012) 112301, arXiv:1205.6443 [hep-ex].
[32] ALICE Collaboration, B. Abelev, et al., D_s^+ meson production at central rapidity in proton–proton collisions at $\sqrt{s} = 7$ TeV, Phys. Lett. B 718 (2012) 279–294, arXiv:1208.1948 [hep-ex].
[33] M. Gyulassy, M. Plümer, Jet quenching as a probe of dense matter, Nucl. Phys. A 527 (0) (1991) 641–644.
[34] X.-N. Wang, M. Gyulassy, M. Plumer, The LPM effect in QCD and radiative energy loss in a quark gluon plasma, Phys. Rev. D 51 (1995) 3436–3446, arXiv:hep-ph/9408344.
[35] R. Baier, Y.L. Dokshitzer, A.H. Mueller, S. Peigne, D. Schiff, Radiative energy loss and $p(T)$ broadening of high-energy partons in nuclei, Nucl. Phys. B 484 (1997) 265–282, arXiv:hep-ph/9608322.
[36] M.H. Thoma, M. Gyulassy, Quark damping and energy loss in the high temperature qcd, Nucl. Phys. B 351 (3) (1991) 491–506.
[37] E. Braaten, M.H. Thoma, Energy loss of a heavy fermion in a hot qed plasma, Phys. Rev. D 44 (Aug 1991) 1298–1310, http://link.aps.org/doi/10.1103/PhysRevD.44.1298.
[38] E. Braaten, M.H. Thoma, Energy loss of a heavy quark in the quark–gluon plasma, Phys. Rev. D 44 (Nov 1991) R2625–R2630, http://link.aps.org/doi/10.1103/PhysRevD.44.R2625.
[39] A. Majumder, Elastic energy loss and longitudinal straggling of a hard jet, Phys. Rev. C 80 (2009) 031902, arXiv:0810.4967 [nucl-th].

[40] Particle Data Group Collaboration, K.A. Olive, et al., Review of particle physics, Chin. Phys. C 38 (2014) 090001.

[41] Y.L. Dokshitzer, D. Kharzeev, Heavy quark colorimetry of QCD matter, Phys. Lett. B 519 (2001) 199–206, arXiv:hep-ph/0106202.

[42] N. Armesto, C.A. Salgado, U.A. Wiedemann, Medium induced gluon radiation off massive quarks fills the dead cone, Phys. Rev. D 69 (2004) 114003, arXiv:hep-ph/0312106.

[43] M. Djordjevic, M. Gyulassy, Heavy quark radiative energy loss in QCD matter, Nucl. Phys. A 733 (2004) 265–298, arXiv:nucl-th/0310076.

[44] B.-W. Zhang, E. Wang, X.-N. Wang, Heavy quark energy loss in a nuclear medium, Phys. Rev. Lett. 93 (Aug 2004) 072301, http://link.aps.org/doi/10.1103/PhysRevLett.93.072301.

[45] S. Wicks, W. Horowitz, M. Djordjevic, M. Gyulassy, Heavy quark jet quenching with collisional plus radiative energy loss and path length fluctuations, Nucl. Phys. A 783 (2007) 493–496, arXiv:nucl-th/0701063.

[46] H. van Hees, V. Greco, R. Rapp, Heavy-quark probes of the quark–gluon plasma at RHIC, Phys. Rev. C 73 (2006) 034913, arXiv:nucl-th/0508055.

[47] ALICE Collaboration, J. Adam, et al., Centrality dependence of high-p_T D meson suppression in Pb–Pb collisions at $\sqrt{s_{\rm NN}} = 2.76$ TeV, J. High Energy Phys. 11 (2015) 205, arXiv:1506.06604 [nucl-ex].

[48] ALICE Collaboration, J. Adam, et al., Transverse momentum dependence of D-meson production in Pb–Pb collisions at $\sqrt{s_{\rm NN}} = 2.76$ TeV, J. High Energy Phys. 03 (2016) 081, arXiv:1509.06888 [nucl-ex].

[49] CMS Collaboration, S. Chatrchyan, et al., Evidence of b-jet quenching in PbPb collisions at $\sqrt{s_{NN}} = 2.76$ TeV, Phys. Rev. Lett. 113 (13) (2014) 132301, arXiv:1312.4198. Erratum: Phys. Rev. Lett. 115 (2) (2015) 029903.

[50] PHENIX Collaboration, A. Adare, et al., System-size dependence of open-heavy-flavor production in nucleus–nucleus collisions at $\sqrt{s_{NN}} = 200$ GeV, Phys. Rev. C 90 (3) (2014) 034903, arXiv:1310.8286 [nucl-ex].

[51] STAR Collaboration, B.I. Abelev, et al., Transverse momentum and centrality dependence of high-p_T non-photonic electron suppression in Au+Au collisions at $\sqrt{s_NN} = 200$ GeV, Phys. Rev. Lett. 98 (2007) 192301, arXiv:nucl-ex/0607012. Erratum: Phys. Rev. Lett. 106 (2011) 159902.

[52] STAR Collaboration, L. Adamczyk, et al., Observation of D^0 meson nuclear modifications in Au+Au collisions at $\sqrt{s_{NN}} = 200$ GeV, Phys. Rev. Lett. 113 (14) (2014) 142301, arXiv:1404.6185 [nucl-ex].

[53] ALICE Collaboration, B. Abelev, et al., Centrality determination of Pb–Pb collisions at $\sqrt{s_{NN}} = 2.76$ TeV with ALICE, Phys. Rev. C 88 (4) (2013) 044909, arXiv:1301.4361 [nucl-ex].

[54] CMS Collaboration, S. Chatrchyan, et al., Measurement of isolated photon production in pp and PbPb collisions at $\sqrt{s_{NN}} = 2.76$ TeV, Phys. Lett. B 710 (2012) 256–277, arXiv:1201.3093 [nucl-ex].

[55] CMS Collaboration, S. Chatrchyan, et al., Study of W boson production in PbPb and pp collisions at $\sqrt{s_{NN}} = 2.76$ TeV, Phys. Lett. B 715 (2012) 66–87, arXiv:1205.6334 [nucl-ex].

[56] CMS Collaboration, S. Chatrchyan, et al., Study of Z boson production in PbPb collisions at $\sqrt{s_{NN}} = 2.76$ TeV, Phys. Rev. Lett. 106 (2011) 212301, arXiv:1102.5435 [nucl-ex].

[57] ATLAS Collaboration, G. Aad, et al., Measurement of Z boson production in Pb+Pb collisions at $\sqrt{s_{\rm NN}} = 2.76$ TeV with the ATLAS detector, Phys. Rev. Lett. 110 (2013) 022301, arXiv:1210.6486 [hep-ex].

[58] ATLAS Collaboration, G. Aad, et al., Measurement of the production and lepton charge asymmetry of W bosons in Pb+Pb collisions at $\sqrt{s_{NN}} = 2.76$ TeV with the ATLAS detector, Eur. Phys. J. C 75 (1) (2015) 23, arXiv:1408.4674 [hep-ex].

[59] ALICE Collaboration, B.B. Abelev, et al., Transverse momentum dependence of inclusive primary charged-particle production in p–Pb collisions at $\sqrt{s_{\rm NN}} = 5.02$ TeV, Eur. Phys. J. C 74 (9) (2014) 3054, arXiv:1405.2737 [nucl-ex].

[60] ALICE Collaboration, B.B. Abelev, et al., Measurement of prompt D-meson production in p–Pb collisions at $\sqrt{s_{NN}} = 5.02$ TeV, Phys. Rev. Lett. 113 (23) (2014) 232301, arXiv:1405.3452 [nucl-ex].

[61] ALICE Collaboration, J. Adam, et al., Measurement of electrons from heavy-flavour hadron decays in p–Pb collisions at $\sqrt{s_{\rm NN}} = 5.02$ TeV, Phys. Lett. B 754 (2016) 81–93, arXiv:1509.07491 [nucl-ex].

[62] L. Evans, P. Bryant, LHC machine, J. Instrum. 3 (2008) S08001.

[63] ALICE Collaboration, K. Aamodt, et al., The ALICE experiment at the CERN LHC, J. Instrum. 3 (2008) S08002.

[64] ALICE Collaboration, B.B. Abelev, et al., Performance of the ALICE experiment at the CERN LHC, Int. J. Mod. Phys. A 29 (2014) 1430044, arXiv:1402.4476 [nucl-ex].

[65] M.L. Miller, K. Reygers, S.J. Sanders, P. Steinberg, Glauber modeling in high energy nuclear collisions, Annu. Rev. Nucl. Part. Sci. 57 (2007) 205–243, arXiv:nucl-ex/0701025.

[66] ALICE Collaboration, B. Abelev, et al., Measurement of electrons from beauty hadron decays in pp collisions at $\sqrt{s} = 7$ TeV, Phys. Lett. B 721 (2013) 13–23, arXiv:1208.1902 [hep-ex].

[67] T. Sjostrand, S. Mrenna, P.Z. Skands, PYTHIA 6.4 physics and manual, J. High Energy Phys. 05 (2006) 026, arXiv:hep-ph/0603175.

[68] X.-N. Wang, M. Gyulassy, HIJING: a Monte Carlo model for multiple jet production in pp, pA and AA collisions, Phys. Rev. D 44 (1991) 3501–3516.

[69] R. Brun, F. Bruyant, M. Maire, A.C. McPherson, P. Zanarini, GEANT3.

[70] F. Bossu, Z.C. del Valle, A. de Falco, M. Gagliardi, S. Grigoryan, G. Martinez Garcia, Phenomenological interpolation of the inclusive J/psi cross section to proton–proton collisions at 2.76 TeV and 5.5 TeV, arXiv:1103.2394 [nucl-ex].

[71] ALICE Collaboration, J. Adam, et al., Inclusive, prompt and non-prompt J/ψ production at mid-rapidity in Pb–Pb collisions at $\sqrt{s_{\rm NN}} = 2.76$ TeV, J. High Energy Phys. 07 (2015) 051, arXiv:1504.07151 [nucl-ex].

[72] ALICE Collaboration, B.B. Abelev, et al., Centrality, rapidity and transverse momentum dependence of J/ψ suppression in Pb–Pb collisions at $\sqrt{s_{\rm NN}} = 2.76$ TeV, Phys. Lett. B 734 (2014) 314–327, arXiv:1311.0214 [nucl-ex].

[73] CMS Collaboration, S. Chatrchyan, et al., Measurement of the $\Upsilon(1S)$, $\Upsilon(2S)$, and $\Upsilon(3S)$ cross sections in pp collisions at $\sqrt{s} = 7$ TeV, Phys. Lett. B 727 (2013) 101–125, arXiv:1303.5900 [hep-ex].

[74] C. Oleari, The POWHEG-BOX, Nucl. Phys. Proc. Suppl. 205–206 (2010) 36–41, arXiv:1007.3893 [hep-ph].

[75] ALICE Collaboration, B. Abelev, et al., Suppression of high transverse momentum D mesons in central Pb–Pb collisions at $\sqrt{s_{NN}} = 2.76$ TeV, J. High Energy Phys. 09 (2012) 112, arXiv:1203.2160 [nucl-ex].

[76] ALICE Collaboration, B. Abelev, et al., Centrality dependence of charged particle production at large transverse momentum in Pb–Pb collisions at $\sqrt{s_{\rm NN}} = 2.76$ TeV, Phys. Lett. B 720 (2013) 52–62, arXiv:1208.2711 [hep-ex].

[77] CMS Collaboration, V. Khachatryan, et al., J/psi results from CMS in PbPb collisions, with 150 μb^{-1} data.

[78] ATLAS Collaboration, G. Aad, et al., Measurements of the W production cross sections in association with jets with the ATLAS detector, Eur. Phys. J. C 75 (2) (2015) 82, arXiv:1409.8639 [hep-ex].

[79] ATLAS Collaboration, G. Aad, et al., Measurement of the low-mass Drell–Yan differential cross section at $\sqrt{s} = 7$ TeV using the ATLAS detector, J. High Energy Phys. 06 (2014) 112, arXiv:1404.1212 [hep-ex].

[80] M. Cacciari, S. Frixione, P. Nason, The $p(T)$ spectrum in heavy flavor photoproduction, J. High Energy Phys. 0103 (2001) 006, arXiv:hep-ph/0102134.

[81] M. Cacciari, S. Frixione, N. Houdeau, M.L. Mangano, P. Nason, G. Ridolfi, Theoretical predictions for charm and bottom production at the LHC, J. High Energy Phys. 10 (2012) 137, arXiv:1205.6344 [hep-ph].

[82] ALICE Collaboration, B. Abelev, et al., Measurement of electrons from semileptonic heavy-flavour hadron decays in pp collisions at $\sqrt{s} = 7$ TeV, Phys. Rev. D 86 (2012) 112007, arXiv:1205.5423 [hep-ex].

[83] ATLAS Collaboration, G. Aad, et al., Measurements of the electron and muon inclusive cross-sections in proton-proton collisions at $\sqrt{s} = 7$ TeV with the ATLAS detector, Phys. Lett. B 707 (2012) 438–458, arXiv:1109.0525 [hep-ex].

[84] R. Averbeck, et al., Reference heavy flavour cross sections in pp collisions at $\sqrt{s} = 2.76$ TeV, using a pQCD-driven $\sqrt{s}$-scaling of ALICE measurements at $\sqrt{s} = 7$ TeV, arXiv:1107.3243 [nucl-ex].

[85] ALICE Collaboration, B.B. Abelev, et al., Beauty production in pp collisions at $\sqrt{s} = 2.76$ TeV measured via semi-electronic decays, Phys. Lett. B 738 (2014) 97–108, arXiv:1405.4144 [nucl-ex].

[86] M. Djordjevic, M. Djordjevic, B. Blagojevic, RHIC and LHC jet suppression in non-central collisions, Phys. Lett. B 737 (2014) 298–302, arXiv:1405.4250 [nucl-th].

[87] S. Wicks, W. Horowitz, M. Djordjevic, M. Gyulassy, Elastic, inelastic, and path length fluctuations in jet tomography, Nucl. Phys. A 784 (2007) 426–442, arXiv:nucl-th/0512076.

[88] W. Horowitz, M. Gyulassy, The surprising transparency of the sQGP at LHC, Nucl. Phys. A 872 (2011) 265–285, arXiv:1104.4958 [hep-ph].

[89] W. Horowitz, Testing pQCD and AdS/CFT energy loss at RHIC and LHC, AIP Conf. Proc. 1441 (2012) 889–891, arXiv:1108.5876 [hep-ph].

[90] R. Sharma, I. Vitev, B.-W. Zhang, Light-cone wave function approach to open heavy flavor dynamics in QCD matter, Phys. Rev. C 80 (2009) 054902, arXiv:0904.0032 [hep-ph].

[91] M. He, R.J. Fries, R. Rapp, Heavy flavor at the large hadron collider in a strong coupling approach, Phys. Lett. B 735 (2014) 445–450, arXiv:1401.3817 [nucl-th].

[92] S. Cao, G.-Y. Qin, S.A. Bass, Heavy-quark dynamics and hadronization in ultra-relativistic heavy-ion collisions: collisional versus radiative energy loss, Phys. Rev. C 88 (4) (2013) 044907, arXiv:1308.0617 [nucl-th].

[93] M. Nahrgang, J. Aichelin, P.B. Gossiaux, K. Werner, Influence of hadronic bound states above T_c on heavy-quark observables in Pb + Pb collisions at at the CERN large hadron collider, Phys. Rev. C 89 (1) (2014) 014905, arXiv:1305.6544 [hep-ph].

[94] W. Alberico, A. Beraudo, A. De Pace, A. Molinari, M. Monteno, et al., Heavy-flavour spectra in high energy nucleus–nucleus collisions, Eur. Phys. J. C 71 (2011) 1666, arXiv:1101.6008 [hep-ph].

[95] A. Beraudo, A. De Pace, M. Monteno, M. Nardi, F. Prino, Heavy flavors in heavy-ion collisions: quenching, flow and correlations, Eur. Phys. J. C 75 (3) (2015) 121, arXiv:1410.6082 [hep-ph].

[96] J. Uphoff, O. Fochler, Z. Xu, C. Greiner, Elliptic flow and energy loss of heavy quarks in ultra-relativistic heavy ion collisions, Phys. Rev. C 84 (2011) 024908, arXiv:1104.2295 [hep-ph].

[97] O. Fochler, J. Uphoff, Z. Xu, C. Greiner, Jet quenching and elliptic flow at RHIC and LHC within a pQCD-based partonic transport model, J. Phys. G 38 (2011) 124152, arXiv:1107.0130 [hep-ph].
[98] J. Uphoff, O. Fochler, Z. Xu, C. Greiner, Open heavy flavor in Pb+Pb collisions at $\sqrt{s} = 2.76$ TeV within a transport model, Phys. Lett. B 717 (2012) 430–435, arXiv:1205.4945 [hep-ph].
[99] ALICE Collaboration, B. Abelev, et al., D meson elliptic flow in non-central Pb–Pb collisions at $\sqrt{s_{\rm NN}} = 2.76$ TeV, Phys. Rev. Lett. 111 (2013) 102301, arXiv:1305.2707 [nucl-ex].
[100] ALICE Collaboration, J. Adam, et al., Elliptic flow of electrons from heavy-flavour hadron decays at mid-rapidity in Pb–Pb collisions at $\sqrt{s_{\rm NN}} = 2.76$ TeV, arXiv:1606.00321 [nucl-ex].
[101] M. Gyulassy, P. Levai, I. Vitev, Reaction operator approach to nonAbelian energy loss, Nucl. Phys. B 594 (2001) 371–419, arXiv:nucl-th/0006010.

ALICE Collaboration

J. Adam [39], D. Adamová [86], M.M. Aggarwal [90], G. Aglieri Rinella [35], M. Agnello [113,31], N. Agrawal [48], Z. Ahammed [137], S. Ahmad [18], S.U. Ahn [70], S. Aiola [141], A. Akindinov [55], S.N. Alam [137], D.S.D. Albuquerque [124], D. Aleksandrov [82], B. Alessandro [113], D. Alexandre [104], R. Alfaro Molina [65], A. Alici [12,107], A. Alkin [3], J. Alme [22,37], T. Alt [42], S. Altinpinar [22], I. Altsybeev [136], C. Alves Garcia Prado [123], M. An [7], C. Andrei [80], H.A. Andrews [104], A. Andronic [100], V. Anguelov [96], C. Anson [89], T. Antičić [101], F. Antinori [110], P. Antonioli [107], R. Anwar [126], L. Aphecetche [116], H. Appelshäuser [61], S. Arcelli [27], R. Arnaldi [113], O.W. Arnold [97,36], I.C. Arsene [21], M. Arslandok [61], B. Audurier [116], A. Augustinus [35], R. Averbeck [100], M.D. Azmi [18], A. Badalà [109], Y.W. Baek [69], S. Bagnasco [113], R. Bailhache [61], R. Bala [93], S. Balasubramanian [141], A. Baldisseri [15], R.C. Baral [58], A.M. Barbano [26], R. Barbera [28], F. Barile [33], G.G. Barnaföldi [140], L.S. Barnby [35,104], V. Barret [72], P. Bartalini [7], K. Barth [35], J. Bartke [120,i], E. Bartsch [61], M. Basile [27], N. Bastid [72], S. Basu [137], B. Bathen [62], G. Batigne [116], A. Batista Camejo [72], B. Batyunya [68], P.C. Batzing [21], I.G. Bearden [83], H. Beck [96], C. Bedda [31], N.K. Behera [51], I. Belikov [66], F. Bellini [27], H. Bello Martinez [2], R. Bellwied [126], L.G.E. Beltran [122], V. Belyaev [77], G. Bencedi [140], S. Beole [26], A. Bercuci [80], Y. Berdnikov [88], D. Berenyi [140], R.A. Bertens [129,54], D. Berzano [35], L. Betev [35], A. Bhasin [93], I.R. Bhat [93], A.K. Bhati [90], B. Bhattacharjee [44], J. Bhom [120], L. Bianchi [126], N. Bianchi [74], C. Bianchin [139], J. Bielčík [39], J. Bielčíková [86], A. Bilandzic [36,97], G. Biro [140], R. Biswas [4], S. Biswas [81,4], S. Bjelogrlic [54], J.T. Blair [121], D. Blau [82], C. Blume [61], F. Bock [76,96], A. Bogdanov [77], L. Boldizsár [140], M. Bombara [40], M. Bonora [35], J. Book [61], H. Borel [15], A. Borissov [99], M. Borri [128], E. Botta [26], C. Bourjau [83], P. Braun-Munzinger [100], M. Bregant [123], T.A. Broker [61], T.A. Browning [98], M. Broz [39], E.J. Brucken [46], E. Bruna [113], G.E. Bruno [33], D. Budnikov [102], H. Buesching [61], S. Bufalino [31,26], P. Buhler [115], S.A.I. Buitron [63], P. Buncic [35], O. Busch [132], Z. Buthelezi [67], J.B. Butt [16], J.T. Buxton [19], J. Cabala [118], D. Caffarri [35], H. Caines [141], A. Caliva [54], E. Calvo Villar [105], P. Camerini [25], F. Carena [35], W. Carena [35], F. Carnesecchi [12,27], J. Castillo Castellanos [15], A.J. Castro [129], E.A.R. Casula [24], C. Ceballos Sanchez [9], J. Cepila [39], P. Cerello [113], J. Cerkala [118], B. Chang [127], S. Chapeland [35], M. Chartier [128], J.L. Charvet [15], S. Chattopadhyay [137], S. Chattopadhyay [103], A. Chauvin [97,36], V. Chelnokov [3], M. Cherney [89], C. Cheshkov [134], B. Cheynis [134], V. Chibante Barroso [35], D.D. Chinellato [124], S. Cho [51], P. Chochula [35], K. Choi [99], M. Chojnacki [83], S. Choudhury [137], P. Christakoglou [84], C.H. Christensen [83], P. Christiansen [34], T. Chujo [132], S.U. Chung [99], C. Cicalo [108], L. Cifarelli [12,27], F. Cindolo [107], J. Cleymans [92], F. Colamaria [33], D. Colella [56,35], A. Collu [76], M. Colocci [27], G. Conesa Balbastre [73], Z. Conesa del Valle [52], M.E. Connors [141,ii], J.G. Contreras [39], T.M. Cormier [87], Y. Corrales Morales [113], I. Cortés Maldonado [2], P. Cortese [32], M.R. Cosentino [123,125], F. Costa [35], J. Crkovská [52], P. Crochet [72], R. Cruz Albino [11], E. Cuautle [63], L. Cunqueiro [35,62], T. Dahms [36,97], A. Dainese [110], M.C. Danisch [96], A. Danu [59], D. Das [103], I. Das [103], S. Das [4], A. Dash [81], S. Dash [48], S. De [49,123], A. De Caro [30], G. de Cataldo [106], C. de Conti [123], J. de Cuveland [42], A. De Falco [24], D. De Gruttola [30,12], N. De Marco [113], S. De Pasquale [30], R.D. De Souza [124], A. Deisting [100,96], A. Deloff [79], C. Deplano [84], P. Dhankher [48], D. Di Bari [33], A. Di Mauro [35], P. Di Nezza [74], B. Di Ruzza [110], M.A. Diaz Corchero [10], T. Dietel [92], P. Dillenseger [61], R. Divià [35], Ø. Djuvsland [22], A. Dobrin [84,35], D. Domenicis Gimenez [123], B. Dönigus [61], O. Dordic [21], T. Drozhzhova [61], A.K. Dubey [137], A. Dubla [100], L. Ducroux [134], A.K. Duggal [90], P. Dupieux [72], R.J. Ehlers [141], D. Elia [106], E. Endress [105], H. Engel [60], E. Epple [141], B. Erazmus [116], F. Erhardt [133], B. Espagnon [52], S. Esumi [132], G. Eulisse [35], J. Eum [99], D. Evans [104], S. Evdokimov [114], G. Eyyubova [39], L. Fabbietti [36,97], D. Fabris [110], J. Faivre [73], A. Fantoni [74], M. Fasel [87,76], L. Feldkamp [62], A. Feliciello [113], G. Feofilov [136], J. Ferencei [86], A. Fernández Téllez [2], E.G. Ferreiro [17], A. Ferretti [26], A. Festanti [29], V.J.G. Feuillard [72,15], J. Figiel [120], M.A.S. Figueredo [123], S. Filchagin [102], D. Finogeev [53], F.M. Fionda [24], E.M. Fiore [33], M. Floris [35], S. Foertsch [67], P. Foka [100], S. Fokin [82], E. Fragiacomo [112], A. Francescon [35], A. Francisco [116], U. Frankenfeld [100], G.G. Fronze [26], U. Fuchs [35], C. Furget [73], A. Furs [53], M. Fusco Girard [30], J.J. Gaardhøje [83],

M. Gagliardi [26], A.M. Gago [105], K. Gajdosova [83], M. Gallio [26], C.D. Galvan [122], D.R. Gangadharan [76], P. Ganoti [91,35], C. Gao [7], C. Garabatos [100], E. Garcia-Solis [13], K. Garg [28], P. Garg [49], C. Gargiulo [35], P. Gasik [97,36], E.F. Gauger [121], M.B. Gay Ducati [64], M. Germain [116], P. Ghosh [137], S.K. Ghosh [4], P. Gianotti [74], P. Giubellino [113,35], P. Giubilato [29], E. Gladysz-Dziadus [120], P. Glässel [96], D.M. Goméz Coral [65], A. Gomez Ramirez [60], A.S. Gonzalez [35], V. Gonzalez [10], P. González-Zamora [10], S. Gorbunov [42], L. Görlich [120], S. Gotovac [119], V. Grabski [65], L.K. Graczykowski [138], K.L. Graham [104], L. Greiner [76], A. Grelli [54], C. Grigoras [35], V. Grigoriev [77], A. Grigoryan [1], S. Grigoryan [68], N. Grion [112], J.M. Gronefeld [100], J.F. Grosse-Oetringhaus [35], R. Grosso [100], L. Gruber [115], F. Guber [53], R. Guernane [73,35], B. Guerzoni [27], K. Gulbrandsen [83], T. Gunji [131], A. Gupta [93], R. Gupta [93], I.B. Guzman [2], R. Haake [35,62], C. Hadjidakis [52], H. Hamagaki [131,78], G. Hamar [140], J.C. Hamon [66], J.W. Harris [141], A. Harton [13], D. Hatzifotiadou [107], S. Hayashi [131], S.T. Heckel [61], E. Hellbär [61], H. Helstrup [37], A. Herghelegiu [80], G. Herrera Corral [11], F. Herrmann [62], B.A. Hess [95], K.F. Hetland [37], H. Hillemanns [35], B. Hippolyte [66], J. Hladky [57], D. Horak [39], R. Hosokawa [132], P. Hristov [35], C. Hughes [129], T.J. Humanic [19], N. Hussain [44], T. Hussain [18], D. Hutter [42], D.S. Hwang [20], R. Ilkaev [102], M. Inaba [132], M. Ippolitov [82,77], M. Irfan [18], V. Isakov [53], M.S. Islam [49], M. Ivanov [35,100], V. Ivanov [88], V. Izucheev [114], B. Jacak [76], N. Jacazio [27], P.M. Jacobs [76], M.B. Jadhav [48], S. Jadlovska [118], J. Jadlovsky [118], C. Jahnke [123,36], M.J. Jakubowska [138], M.A. Janik [138], P.H.S.Y. Jayarathna [126], C. Jena [81], S. Jena [126], R.T. Jimenez Bustamante [100], P.G. Jones [104], A. Jusko [104], P. Kalinak [56], A. Kalweit [35], J.H. Kang [142], V. Kaplin [77], S. Kar [137], A. Karasu Uysal [71], O. Karavichev [53], T. Karavicheva [53], L. Karayan [100,96], E. Karpechev [53], U. Kebschull [60], R. Keidel [143], D.L.D. Keijdener [54], M. Keil [35], M. Mohisin Khan [18,iii], P. Khan [103], S.A. Khan [137], A. Khanzadeev [88], Y. Kharlov [114], A. Khatun [18], A. Khuntia [49], B. Kileng [37], D.W. Kim [43], D.J. Kim [127], D. Kim [142], H. Kim [142], J.S. Kim [43], J. Kim [96], M. Kim [51], M. Kim [142], S. Kim [20], T. Kim [142], S. Kirsch [42], I. Kisel [42], S. Kiselev [55], A. Kisiel [138], G. Kiss [140], J.L. Klay [6], C. Klein [61], J. Klein [35], C. Klein-Bösing [62], S. Klewin [96], A. Kluge [35], M.L. Knichel [96], A.G. Knospe [121,126], C. Kobdaj [117], M. Kofarago [35], T. Kollegger [100], A. Kolojvari [136], V. Kondratiev [136], N. Kondratyeva [77], E. Kondratyuk [114], A. Konevskikh [53], M. Kopcik [118], M. Kour [93], C. Kouzinopoulos [35], O. Kovalenko [79], V. Kovalenko [136], M. Kowalski [120], G. Koyithatta Meethaleveedu [48], I. Králik [56], A. Kravčáková [40], M. Krivda [104,56], F. Krizek [86], E. Kryshen [88,35], M. Krzewicki [42], A.M. Kubera [19], V. Kučera [86], C. Kuhn [66], P.G. Kuijer [84], A. Kumar [93], J. Kumar [48], L. Kumar [90], S. Kumar [48], S. Kundu [81], P. Kurashvili [79], A. Kurepin [53], A.B. Kurepin [53], A. Kuryakin [102], S. Kushpil [86], M.J. Kweon [51], Y. Kwon [142], S.L. La Pointe [42], P. La Rocca [28], C. Lagana Fernandes [123], I. Lakomov [35], R. Langoy [41], K. Lapidus [36,141], C. Lara [60], A. Lardeux [15], A. Lattuca [26], E. Laudi [35], L. Lazaridis [35], R. Lea [25], L. Leardini [96], S. Lee [142], F. Lehas [84], S. Lehner [115], J. Lehrbach [42], R.C. Lemmon [85], V. Lenti [106], E. Leogrande [54], I. León Monzón [122], P. Lévai [140], S. Li [7], X. Li [14], J. Lien [41], R. Lietava [104], S. Lindal [21], V. Lindenstruth [42], C. Lippmann [100], M.A. Lisa [19], H.M. Ljunggren [34], W. Llope [139], D.F. Lodato [54], P.I. Loenne [22], V. Loginov [77], C. Loizides [76], X. Lopez [72], E. López Torres [9], A. Lowe [140], P. Luettig [61], M. Lunardon [29], G. Luparello [25], M. Lupi [35], T.H. Lutz [141], A. Maevskaya [53], M. Mager [35], S. Mahajan [93], S.M. Mahmood [21], A. Maire [66], R.D. Majka [141], M. Malaev [88], I. Maldonado Cervantes [63], L. Malinina [68,iv], D. Mal'Kevich [55], P. Malzacher [100], A. Mamonov [102], V. Manko [82], F. Manso [72], V. Manzari [106], Y. Mao [7], M. Marchisone [67,130], J. Mareš [57], G.V. Margagliotti [25], A. Margotti [107], J. Margutti [54], A. Marín [100], C. Markert [121], M. Marquard [61], N.A. Martin [100], P. Martinengo [35], M.I. Martínez [2], G. Martínez García [116], M. Martinez Pedreira [35], A. Mas [123], S. Masciocchi [100], M. Masera [26], A. Masoni [108], A. Mastroserio [33], A. Matyja [120,129], C. Mayer [120], J. Mazer [129], M. Mazzilli [33], M.A. Mazzoni [111], F. Meddi [23], Y. Melikyan [77], A. Menchaca-Rocha [65], E. Meninno [30], J. Mercado Pérez [96], M. Meres [38], S. Mhlanga [92], Y. Miake [132], M.M. Mieskolainen [46], K. Mikhaylov [55,68], L. Milano [76], J. Milosevic [21], A. Mischke [54], A.N. Mishra [49], T. Mishra [58], D. Miśkowiec [100], J. Mitra [137], C.M. Mitu [59], N. Mohammadi [54], B. Mohanty [81], L. Molnar [116], E. Montes [10], D.A. Moreira De Godoy [62], L.A.P. Moreno [2], S. Moretto [29], A. Morreale [116], A. Morsch [35], V. Muccifora [74], E. Mudnic [119], D. Mühlheim [62], S. Muhuri [137], M. Mukherjee [137], J.D. Mulligan [141], M.G. Munhoz [123], K. Münning [45], R.H. Munzer [97,61,36], H. Murakami [131], S. Murray [67], L. Musa [35], J. Musinsky [56], C.J. Myers [126], B. Naik [48], R. Nair [79], B.K. Nandi [48], R. Nania [107], E. Nappi [106], M.U. Naru [16], H. Natal da Luz [123], C. Nattrass [129], S.R. Navarro [2], K. Nayak [81], R. Nayak [48], T.K. Nayak [137], S. Nazarenko [102], A. Nedosekin [55], R.A. Negrao De Oliveira [35], L. Nellen [63], F. Ng [126], M. Nicassio [100], M. Niculescu [59], J. Niedziela [35], B.S. Nielsen [83], S. Nikolaev [82], S. Nikulin [82], V. Nikulin [88], F. Noferini [12,107],

P. Nomokonov [68], G. Nooren [54], J.C.C. Noris [2], J. Norman [128], A. Nyanin [82], J. Nystrand [22], H. Oeschler [96], S. Oh [141], A. Ohlson [35], T. Okubo [47], L. Olah [140], J. Oleniacz [138], A.C. Oliveira Da Silva [123], M.H. Oliver [141], J. Onderwaater [100], C. Oppedisano [113], R. Orava [46], M. Oravec [118], A. Ortiz Velasquez [63], A. Oskarsson [34], J. Otwinowski [120], K. Oyama [78], M. Ozdemir [61], Y. Pachmayer [96], V. Pacik [83], D. Pagano [135,26], P. Pagano [30], G. Paić [63], S.K. Pal [137], P. Palni [7], J. Pan [139], A.K. Pandey [48], V. Papikyan [1], G.S. Pappalardo [109], P. Pareek [49], J. Park [51], W.J. Park [100], S. Parmar [90], A. Passfeld [62], V. Paticchio [106], R.N. Patra [137], B. Paul [113], H. Pei [7], T. Peitzmann [54], X. Peng [7], H. Pereira Da Costa [15], D. Peresunko [77,82], E. Perez Lezama [61], V. Peskov [61], Y. Pestov [5], V. Petráček [39], V. Petrov [114], M. Petrovici [80], C. Petta [28], S. Piano [112], M. Pikna [38], P. Pillot [116], L.O.D.L. Pimentel [83], O. Pinazza [35,107], L. Pinsky [126], D.B. Piyarathna [126], M. Płoskoń [76], M. Planinic [133], J. Pluta [138], S. Pochybova [140], P.L.M. Podesta-Lerma [122], M.G. Poghosyan [87], B. Polichtchouk [114], N. Poljak [133], W. Poonsawat [117], A. Pop [80], H. Poppenborg [62], S. Porteboeuf-Houssais [72], J. Porter [76], J. Pospisil [86], V. Pozdniakov [68], S.K. Prasad [4], R. Preghenella [107,35], F. Prino [113], C.A. Pruneau [139], I. Pshenichnov [53], M. Puccio [26], G. Puddu [24], P. Pujahari [139], V. Punin [102], J. Putschke [139], H. Qvigstad [21], A. Rachevski [112], S. Raha [4], S. Rajput [93], J. Rak [127], A. Rakotozafindrabe [15], L. Ramello [32], F. Rami [66], D.B. Rana [126], R. Raniwala [94], S. Raniwala [94], S.S. Räsänen [46], B.T. Rascanu [61], D. Rathee [90], V. Ratza [45], I. Ravasenga [26], K.F. Read [87,129], K. Redlich [79], A. Rehman [22], P. Reichelt [61], F. Reidt [35,96], X. Ren [7], R. Renfordt [61], A.R. Reolon [74], A. Reshetin [53], K. Reygers [96], V. Riabov [88], R.A. Ricci [75], T. Richert [34,54], M. Richter [21], P. Riedler [35], W. Riegler [35], F. Riggi [28], C. Ristea [59], M. Rodríguez Cahuantzi [2], K. Røed [21], E. Rogochaya [68], D. Rohr [42], D. Röhrich [22], F. Ronchetti [74,35], L. Ronflette [116], P. Rosnet [72], A. Rossi [29], F. Roukoutakis [91], A. Roy [49], C. Roy [66], P. Roy [103], A.J. Rubio Montero [10], R. Rui [25], R. Russo [26], E. Ryabinkin [82], Y. Ryabov [88], A. Rybicki [120], S. Saarinen [46], S. Sadhu [137], S. Sadovsky [114], K. Šafařík [35], B. Sahlmuller [61], B. Sahoo [48], P. Sahoo [49], R. Sahoo [49], S. Sahoo [58], P.K. Sahu [58], J. Saini [137], S. Sakai [132,74], M.A. Saleh [139], J. Salzwedel [19], S. Sambyal [93], V. Samsonov [77,88], A. Sandoval [65], M. Sano [132], D. Sarkar [137], N. Sarkar [137], P. Sarma [44], M.H.P. Sas [54], E. Scapparone [107], F. Scarlassara [29], R.P. Scharenberg [98], C. Schiaua [80], R. Schicker [96], C. Schmidt [100], H.R. Schmidt [95], M. Schmidt [95], J. Schukraft [35], Y. Schutz [116,66,35], K. Schwarz [100], K. Schweda [100], G. Scioli [27], E. Scomparin [113], R. Scott [129], M. Šefčík [40], J.E. Seger [89], Y. Sekiguchi [131], D. Sekihata [47], I. Selyuzhenkov [100], K. Senosi [67], S. Senyukov [3,35], E. Serradilla [10,65], P. Sett [48], A. Sevcenco [59], A. Shabanov [53], A. Shabetai [116], O. Shadura [3], R. Shahoyan [35], A. Shangaraev [114], A. Sharma [93], A. Sharma [90], M. Sharma [93], M. Sharma [93], N. Sharma [90,129], A.I. Sheikh [137], K. Shigaki [47], Q. Shou [7], K. Shtejer [9,26], Y. Sibiriak [82], S. Siddhanta [108], K.M. Sielewicz [35], T. Siemiarczuk [79], D. Silvermyr [34], C. Silvestre [73], G. Simatovic [133], G. Simonetti [35], R. Singaraju [137], R. Singh [81], V. Singhal [137], T. Sinha [103], B. Sitar [38], M. Sitta [32], T.B. Skaali [21], M. Slupecki [127], N. Smirnov [141], R.J.M. Snellings [54], T.W. Snellman [127], J. Song [99], M. Song [142], Z. Song [7], F. Soramel [29], S. Sorensen [129], F. Sozzi [100], E. Spiriti [74], I. Sputowska [120], B.K. Srivastava [98], J. Stachel [96], I. Stan [59], P. Stankus [87], E. Stenlund [34], G. Steyn [67], J.H. Stiller [96], D. Stocco [116], P. Strmen [38], A.A.P. Suaide [123], T. Sugitate [47], C. Suire [52], M. Suleymanov [16], M. Suljic [25], R. Sultanov [55], M. Šumbera [86], S. Sumowidagdo [50], K. Suzuki [115], S. Swain [58], A. Szabo [38], I. Szarka [38], A. Szczepankiewicz [138], M. Szymanski [138], U. Tabassam [16], J. Takahashi [124], G.J. Tambave [22], N. Tanaka [132], M. Tarhini [52], M. Tariq [18], M.G. Tarzila [80], A. Tauro [35], G. Tejeda Muñoz [2], A. Telesca [35], K. Terasaki [131], C. Terrevoli [29], B. Teyssier [134], D. Thakur [49], D. Thomas [121], R. Tieulent [134], A. Tikhonov [53], A.R. Timmins [126], A. Toia [61], S. Tripathy [49], S. Trogolo [26], G. Trombetta [33], V. Trubnikov [3], W.H. Trzaska [127], T. Tsuji [131], A. Tumkin [102], R. Turrisi [110], T.S. Tveter [21], K. Ullaland [22], E.N. Umaka [126], A. Uras [134], G.L. Usai [24], A. Utrobicic [133], M. Vala [56], J. Van Der Maarel [54], J.W. Van Hoorne [35], M. van Leeuwen [54], T. Vanat [86], P. Vande Vyvre [35], D. Varga [140], A. Vargas [2], M. Vargyas [127], R. Varma [48], M. Vasileiou [91], A. Vasiliev [82], A. Vauthier [73], O. Vázquez Doce [36,97], V. Vechernin [136], A.M. Veen [54], A. Velure [22], E. Vercellin [26], S. Vergara Limón [2], R. Vernet [8], R. Vértesi [140], L. Vickovic [119], S. Vigolo [54], J. Viinikainen [127], Z. Vilakazi [130], O. Villalobos Baillie [104], A. Villatoro Tello [2], A. Vinogradov [82], L. Vinogradov [136], T. Virgili [30], V. Vislavicius [34], A. Vodopyanov [68], M.A. Völkl [96], K. Voloshin [55], S.A. Voloshin [139], G. Volpe [140,33], B. von Haller [35], I. Vorobyev [36,97], D. Voscek [118], D. Vranic [35,100], J. Vrláková [40], B. Wagner [22], J. Wagner [100], H. Wang [54], M. Wang [7], D. Watanabe [132], Y. Watanabe [131], M. Weber [115], S.G. Weber [100], D.F. Weiser [96], J.P. Wessels [62], U. Westerhoff [62], A.M. Whitehead [92], J. Wiechula [61], J. Wikne [21], G. Wilk [79], J. Wilkinson [96], G.A. Willems [62], M.C.S. Williams [107], B. Windelband [96], M. Winn [96], W.E. Witt [129], S. Yalcin [71], P. Yang [7], S. Yano [47], Z. Yin [7],

H. Yokoyama [132,73], I.-K. Yoo [35,99], J.H. Yoon [51], V. Yurchenko [3], V. Zaccolo [83], A. Zaman [16], C. Zampolli [35,107], H.J.C. Zanoli [123], S. Zaporozhets [68], N. Zardoshti [104], A. Zarochentsev [136], P. Závada [57], N. Zaviyalov [102], H. Zbroszczyk [138], M. Zhalov [88], H. Zhang [7,22], X. Zhang [76,7], Y. Zhang [7], C. Zhang [54], Z. Zhang [7], C. Zhao [21], N. Zhigareva [55], D. Zhou [7], Y. Zhou [83], Z. Zhou [22], H. Zhu [7,22], J. Zhu [116,7], A. Zichichi [12,27], A. Zimmermann [96], M.B. Zimmermann [62,35], G. Zinovjev [3], J. Zmeskal [115]

[1] *A.I. Alikhanyan National Science Laboratory (Yerevan Physics Institute) Foundation, Yerevan, Armenia*
[2] *Benemérita Universidad Autónoma de Puebla, Puebla, Mexico*
[3] *Bogolyubov Institute for Theoretical Physics, Kiev, Ukraine*
[4] *Bose Institute, Department of Physics and Centre for Astroparticle Physics and Space Science (CAPSS), Kolkata, India*
[5] *Budker Institute for Nuclear Physics, Novosibirsk, Russia*
[6] *California Polytechnic State University, San Luis Obispo, CA, United States*
[7] *Central China Normal University, Wuhan, China*
[8] *Centre de Calcul de l'IN2P3, Villeurbanne, Lyon, France*
[9] *Centro de Aplicaciones Tecnológicas y Desarrollo Nuclear (CEADEN), Havana, Cuba*
[10] *Centro de Investigaciones Energéticas Medioambientales y Tecnológicas (CIEMAT), Madrid, Spain*
[11] *Centro de Investigación y de Estudios Avanzados (CINVESTAV), Mexico City and Mérida, Mexico*
[12] *Centro Fermi – Museo Storico della Fisica e Centro Studi e Ricerche "Enrico Fermi", Rome, Italy*
[13] *Chicago State University, Chicago, IL, United States*
[14] *China Institute of Atomic Energy, Beijing, China*
[15] *Commissariat à l'Energie Atomique, IRFU, Saclay, France*
[16] *COMSATS Institute of Information Technology (CIIT), Islamabad, Pakistan*
[17] *Departamento de Física de Partículas and IGFAE, Universidad de Santiago de Compostela, Santiago de Compostela, Spain*
[18] *Department of Physics, Aligarh Muslim University, Aligarh, India*
[19] *Department of Physics, Ohio State University, Columbus, OH, United States*
[20] *Department of Physics, Sejong University, Seoul, South Korea*
[21] *Department of Physics, University of Oslo, Oslo, Norway*
[22] *Department of Physics and Technology, University of Bergen, Bergen, Norway*
[23] *Dipartimento di Fisica dell'Università 'La Sapienza' and Sezione INFN, Rome, Italy*
[24] *Dipartimento di Fisica dell'Università and Sezione INFN, Cagliari, Italy*
[25] *Dipartimento di Fisica dell'Università and Sezione INFN, Trieste, Italy*
[26] *Dipartimento di Fisica dell'Università and Sezione INFN, Turin, Italy*
[27] *Dipartimento di Fisica e Astronomia dell'Università and Sezione INFN, Bologna, Italy*
[28] *Dipartimento di Fisica e Astronomia dell'Università and Sezione INFN, Catania, Italy*
[29] *Dipartimento di Fisica e Astronomia dell'Università and Sezione INFN, Padova, Italy*
[30] *Dipartimento di Fisica 'E.R. Caianiello' dell'Università and Gruppo Collegato INFN, Salerno, Italy*
[31] *Dipartimento DISAT del Politecnico and Sezione INFN, Turin, Italy*
[32] *Dipartimento di Scienze e Innovazione Tecnologica dell'Università del Piemonte Orientale and INFN Sezione di Torino, Alessandria, Italy*
[33] *Dipartimento Interateneo di Fisica 'M. Merlin' and Sezione INFN, Bari, Italy*
[34] *Division of Experimental High Energy Physics, University of Lund, Lund, Sweden*
[35] *European Organization for Nuclear Research (CERN), Geneva, Switzerland*
[36] *Excellence Cluster Universe, Technische Universität München, Munich, Germany*
[37] *Faculty of Engineering, Bergen University College, Bergen, Norway*
[38] *Faculty of Mathematics, Physics and Informatics, Comenius University, Bratislava, Slovakia*
[39] *Faculty of Nuclear Sciences and Physical Engineering, Czech Technical University in Prague, Prague, Czech Republic*
[40] *Faculty of Science, P.J. Šafárik University, Košice, Slovakia*
[41] *Faculty of Technology, Buskerud and Vestfold University College, Tonsberg, Norway*
[42] *Frankfurt Institute for Advanced Studies, Johann Wolfgang Goethe-Universität Frankfurt, Frankfurt, Germany*
[43] *Gangneung-Wonju National University, Gangneung, South Korea*
[44] *Gauhati University, Department of Physics, Guwahati, India*
[45] *Helmholtz-Institut für Strahlen- und Kernphysik, Rheinische Friedrich-Wilhelms-Universität Bonn, Bonn, Germany*
[46] *Helsinki Institute of Physics (HIP), Helsinki, Finland*
[47] *Hiroshima University, Hiroshima, Japan*
[48] *Indian Institute of Technology Bombay (IIT), Mumbai, India*
[49] *Indian Institute of Technology Indore, Indore, India*
[50] *Indonesian Institute of Sciences, Jakarta, Indonesia*
[51] *Inha University, Incheon, South Korea*
[52] *Institut de Physique Nucléaire d'Orsay (IPNO), Université Paris-Sud, CNRS-IN2P3, Orsay, France*
[53] *Institute for Nuclear Research, Academy of Sciences, Moscow, Russia*
[54] *Institute for Subatomic Physics of Utrecht University, Utrecht, Netherlands*
[55] *Institute for Theoretical and Experimental Physics, Moscow, Russia*
[56] *Institute of Experimental Physics, Slovak Academy of Sciences, Košice, Slovakia*
[57] *Institute of Physics, Academy of Sciences of the Czech Republic, Prague, Czech Republic*
[58] *Institute of Physics, Bhubaneswar, India*
[59] *Institute of Space Science (ISS), Bucharest, Romania*
[60] *Institut für Informatik, Johann Wolfgang Goethe-Universität Frankfurt, Frankfurt, Germany*
[61] *Institut für Kernphysik, Johann Wolfgang Goethe-Universität Frankfurt, Frankfurt, Germany*
[62] *Institut für Kernphysik, Westfälische Wilhelms-Universität Münster, Münster, Germany*
[63] *Instituto de Ciencias Nucleares, Universidad Nacional Autónoma de México, Mexico City, Mexico*
[64] *Instituto de Física, Universidade Federal do Rio Grande do Sul (UFRGS), Porto Alegre, Brazil*
[65] *Instituto de Física, Universidad Nacional Autónoma de México, Mexico City, Mexico*
[66] *Institut Pluridisciplinaire Hubert Curien (IPHC), Université de Strasbourg, CNRS-IN2P3, Strasbourg, France*
[67] *iThemba LABS, National Research Foundation, Somerset West, South Africa*
[68] *Joint Institute for Nuclear Research (JINR), Dubna, Russia*
[69] *Konkuk University, Seoul, South Korea*
[70] *Korea Institute of Science and Technology Information, Daejeon, South Korea*
[71] *KTO Karatay University, Konya, Turkey*

[72] Laboratoire de Physique Corpusculaire (LPC), Clermont Université, Université Blaise Pascal, CNRS-IN2P3, Clermont-Ferrand, France
[73] Laboratoire de Physique Subatomique et de Cosmologie, Université Grenoble-Alpes, CNRS-IN2P3, Grenoble, France
[74] Laboratori Nazionali di Frascati, INFN, Frascati, Italy
[75] Laboratori Nazionali di Legnaro, INFN, Legnaro, Italy
[76] Lawrence Berkeley National Laboratory, Berkeley, CA, United States
[77] Moscow Engineering Physics Institute, Moscow, Russia
[78] Nagasaki Institute of Applied Science, Nagasaki, Japan
[79] National Centre for Nuclear Studies, Warsaw, Poland
[80] National Institute for Physics and Nuclear Engineering, Bucharest, Romania
[81] National Institute of Science Education and Research, Bhubaneswar, India
[82] National Research Centre Kurchatov Institute, Moscow, Russia
[83] Niels Bohr Institute, University of Copenhagen, Copenhagen, Denmark
[84] Nikhef, Nationaal instituut voor subatomaire fysica, Amsterdam, Netherlands
[85] Nuclear Physics Group, STFC Daresbury Laboratory, Daresbury, United Kingdom
[86] Nuclear Physics Institute, Academy of Sciences of the Czech Republic, Řež u Prahy, Czech Republic
[87] Oak Ridge National Laboratory, Oak Ridge, TN, United States
[88] Petersburg Nuclear Physics Institute, Gatchina, Russia
[89] Physics Department, Creighton University, Omaha, NE, United States
[90] Physics Department, Panjab University, Chandigarh, India
[91] Physics Department, University of Athens, Athens, Greece
[92] Physics Department, University of Cape Town, Cape Town, South Africa
[93] Physics Department, University of Jammu, Jammu, India
[94] Physics Department, University of Rajasthan, Jaipur, India
[95] Physikalisches Institut, Eberhard Karls Universität Tübingen, Tübingen, Germany
[96] Physikalisches Institut, Ruprecht-Karls-Universität Heidelberg, Heidelberg, Germany
[97] Physik Department, Technische Universität München, Munich, Germany
[98] Purdue University, West Lafayette, IN, United States
[99] Pusan National University, Pusan, South Korea
[100] Research Division and ExtreMe Matter Institute EMMI, GSI Helmholtzzentrum für Schwerionenforschung, Darmstadt, Germany
[101] Rudjer Bošković Institute, Zagreb, Croatia
[102] Russian Federal Nuclear Center (VNIIEF), Sarov, Russia
[103] Saha Institute of Nuclear Physics, Kolkata, India
[104] School of Physics and Astronomy, University of Birmingham, Birmingham, United Kingdom
[105] Sección Física, Departamento de Ciencias, Pontificia Universidad Católica del Perú, Lima, Peru
[106] Sezione INFN, Bari, Italy
[107] Sezione INFN, Bologna, Italy
[108] Sezione INFN, Cagliari, Italy
[109] Sezione INFN, Catania, Italy
[110] Sezione INFN, Padova, Italy
[111] Sezione INFN, Rome, Italy
[112] Sezione INFN, Trieste, Italy
[113] Sezione INFN, Turin, Italy
[114] SSC IHEP of NRC Kurchatov institute, Protvino, Russia
[115] Stefan Meyer Institut für Subatomare Physik (SMI), Vienna, Austria
[116] SUBATECH, Ecole des Mines de Nantes, Université de Nantes, CNRS-IN2P3, Nantes, France
[117] Suranaree University of Technology, Nakhon Ratchasima, Thailand
[118] Technical University of Košice, Košice, Slovakia
[119] Technical University of Split FESB, Split, Croatia
[120] The Henryk Niewodniczanski Institute of Nuclear Physics, Polish Academy of Sciences, Cracow, Poland
[121] The University of Texas at Austin, Physics Department, Austin, TX, United States
[122] Universidad Autónoma de Sinaloa, Culiacán, Mexico
[123] Universidade de São Paulo (USP), São Paulo, Brazil
[124] Universidade Estadual de Campinas (UNICAMP), Campinas, Brazil
[125] Universidade Federal do ABC, Santo Andre, Brazil
[126] University of Houston, Houston, TX, United States
[127] University of Jyväskylä, Jyväskylä, Finland
[128] University of Liverpool, Liverpool, United Kingdom
[129] University of Tennessee, Knoxville, TN, United States
[130] University of the Witwatersrand, Johannesburg, South Africa
[131] University of Tokyo, Tokyo, Japan
[132] University of Tsukuba, Tsukuba, Japan
[133] University of Zagreb, Zagreb, Croatia
[134] Université de Lyon, Université Lyon 1, CNRS/IN2P3, IPN-Lyon, Villeurbanne, Lyon, France
[135] Università di Brescia, Brescia, Italy
[136] V. Fock Institute for Physics, St. Petersburg State University, St. Petersburg, Russia
[137] Variable Energy Cyclotron Centre, Kolkata, India
[138] Warsaw University of Technology, Warsaw, Poland
[139] Wayne State University, Detroit, MI, United States
[140] Wigner Research Centre for Physics, Hungarian Academy of Sciences, Budapest, Hungary
[141] Yale University, New Haven, CT, United States
[142] Yonsei University, Seoul, South Korea
[143] Zentrum für Technologietransfer und Telekommunikation (ZTT), Fachhochschule Worms, Worms, Germany

[i] Deceased.
[ii] Also at: Georgia State University, Atlanta, Georgia, United States.
[iii] Also at: Department of Applied Physics, Aligarh Muslim University, Aligarh, India.
[iv] Also at: M.V. Lomonosov Moscow State University, D.V. Skobeltsyn Institute of Nuclear Physics, Moscow, Russia.